

MMLU-Reason: Benchmarking Multi-Task Multi-modal Language Understanding and Reasoning

Guiyao Tie¹ Xueyang Zhou¹ Tianhe Gu¹ Ruihang Zhang¹ Chaoran Hu¹ Sizhe Zhang¹
Mengqu Sun² Yan Zhang¹ Pan Zhou¹ Lichao Sun²

¹Huazhong University of Science and Technology ²Lehigh University

{tgy, d202480819, u202211961, u202211917, u202314532, U202312332}@hust.edu.cn
mes225@lehigh.edu, {u202312543, panzhou}@hust.edu.cn, lis221@lehigh.edu

Abstract

Recent advances in Multi-Modal Large Language Models (MLLMs) have enabled unified processing of language, vision, and structured inputs, opening the door to complex tasks such as logical deduction, spatial reasoning, and scientific analysis. Despite their promise, the reasoning capabilities of MLLMs—particularly those augmented with intermediate thinking traces (MLLMs-T)—remain poorly understood and lack standardized evaluation benchmarks. Existing work focuses primarily on perception or final answer correctness, offering limited insight into how models reason or fail across modalities. To address this gap, we introduce the **MMLU-Reason**, a new benchmark designed to rigorously evaluate multi-modal reasoning with explicit thinking. The **MMLU-Reason** comprises 1) a high-difficulty dataset of 1,083 questions spanning six diverse reasoning types with symbolic depth and multi-hop demands and 2) a modular Reasoning Trace Evaluation Pipeline (RTEP) for assessing reasoning quality beyond accuracy through metrics like relevance, consistency, and structured error annotations. Empirical results show that MLLMs-T overall outperform non-thinking counterparts, but even top models like Claude-3.7-Sonnet and Gemini-2.5 Pro suffer from reasoning pathologies such as inconsistency and overthinking. This benchmark reveals persistent gaps between accuracy and reasoning quality and provides an actionable evaluation pipeline for future model development. Overall, the **MMLU-Reason** offers a scalable foundation for evaluating, comparing, and improving the next generation of multi-modal reasoning systems. Project Page: <https://mmlmr-benchmark.github.io/>.

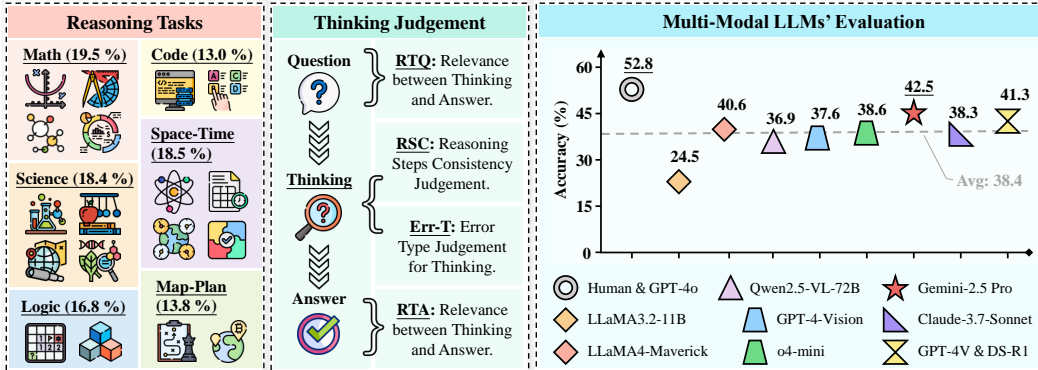


Figure 1: Overview of the **MMLU-Reason**. Left: Six reasoning tasks. Middle: Thinking Judgements assessing alignment for relevance (RTQ, RTA), consistency (RSC), and error (Err-T). Right: Accuracy distribution shows a gap between humans and state-of-the-art MLLMs-T.

1 Introduction

The rapid advancement of Multi-Modal Large Language Models (MLLMs) has significantly enhanced unified reasoning capabilities across language, vision, and structured data modalities. Early MLLMs such as Qwen-VL [8], LLaVA [24], and GPT-4 Vision [35] have demonstrated impressive performance in perception-centric tasks, including visual question answering [7], image captioning [38], and grounded retrieval [37]. However, their proficiency remains limited in tasks necessitating structured reasoning, symbolic abstraction, or sequential multi-step inference. To address this limitation, a new paradigm—MLLMs incorporating explicit intermediate reasoning (MLLMs-T)—has emerged. Representative models such as Gemini-2.5 Pro [13] and Claude-3.7-Sonnet [6] leverage Chain-of-Thought-style reasoning, decomposing complex problems into interpretable intermediate steps, thereby emulating human-like structured problem-solving in domains such as logical deduction, scientific analysis, and code reasoning.

Despite significant progress, rigorously evaluating the reasoning capabilities of MLLMs-T remains challenging. Current benchmarks, including MMBench [30], MME-CoT [18], and MMMU [47], predominantly emphasize broad coverage of tasks and perceptual understanding, offering limited insights into the reasoning process itself. These benchmarks primarily focus on answer correctness without assessing the underlying reasoning’s consistency, coherence, or cognitive alignment. Consequently, a critical research question arises: *To what extent do MLLMs-T reliably generate coherent, interpretable, and cognitively aligned reasoning traces in complex multi-modal tasks?*

Addressing this research question demands a benchmark emphasizing reasoning depth rather than breadth, evaluating not only final predictions but also the intermediate reasoning processes explicitly. Such a benchmark requires 1) challenging multi-modal reasoning tasks explicitly designed to probe structured inference capabilities, and 2) robust criteria for systematically evaluating intermediate reasoning quality. Currently, no benchmark adequately fulfills these requirements [30, 18, 47, 31], leaving a significant gap in diagnosing and attributing reasoning failures at the trace level.

To bridge this gap, we introduce **MMLU-Reason**, a comprehensive benchmark explicitly designed to evaluate the multi-modal reasoning capabilities of both MLLMs and MLLMs-T. As shown in Figure 1, our benchmark comprises 1,083 rigorously curated high-difficulty tasks spanning six reasoning domains: logical reasoning [18, 43], mathematical problem-solving [31, 15], spatio-temporal understanding [18, 44], code reasoning [22, 21], map-based planning [29, 28], and scientific analysis [18, 47]. Each task integrates diverse modalities, including text, images, tables, and diagrams, carefully designed to require structured, symbolic, and abstract reasoning beyond mere perception.

Unlike prior benchmarks [30, 47, 31], **MMLU-Reason** introduces a structured *Reasoning Trace Evaluation Pipeline (RTEP)*, capturing reasoning trace relevance, logical consistency, and frequent error types. This structured evaluation identifies key reasoning pitfalls such as overthinking, trace inconsistency, and logical errors. The right panel of Figure 1 reveals a pronounced performance gap between state-of-the-art MLLMs-T and human-level expert reasoning. Specifically, while the best-performing model, Gemini-2.5 Pro, achieves a test accuracy of 42.45%, human experts assisted by GPT-4o reach 52.85%. This 10.3% margin underscores the persistent challenge in closing the reasoning gap, even with advanced architectures and explicit thinking mechanisms.

In summary, our contributions include:

- **A comprehensive benchmark for multi-modal reasoning.** We introduce **MMLU-Reason**, the first benchmark that systematically targets *multi-modal reasoning* across six domains—Logic, Math, Code, Map, Science, and Space-Time. Unlike prior datasets, **MMLU-Reason** emphasizes hard question solutions and cross-modal alignment to increase reasoning complexity.
- **The first evaluation pipeline for thinking of MLLMs-T.** We propose the Reasoning Trace Evaluation Pipeline (RTEP), the first framework to incorporate intermediate *thinking trace* analysis into multi-modal reasoning evaluation. RTEP assesses reasoning relevance, stepwise consistency, and alignment, which enables deeper diagnostic insight beyond accuracy.
- **Insights into reasoning capabilities and failures.** Through extensive evaluation on **MMLU-Reason**, we find that state-of-the-art MLLMs-T achieve high answer accuracy across tasks, yet frequently produce flawed reasoning traces—exhibiting logical inconsistency or overthinking. These findings expose a critical misalignment between surface-level

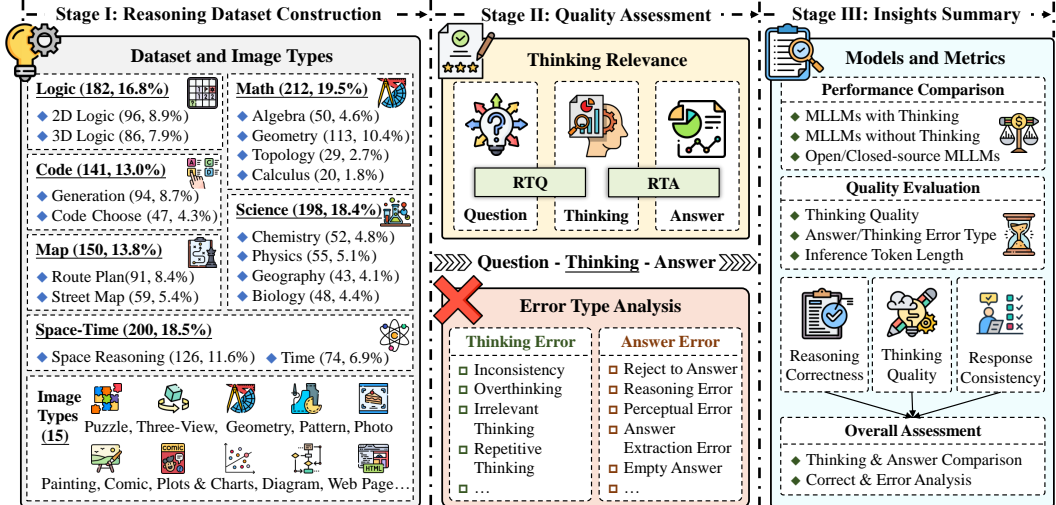


Figure 2: Overview of the **MMLU-Reason** evaluation pipeline. Stage I involves the creation of a challenging multi-modal reasoning benchmark dataset. Stage II evaluates the quality and structural integrity of intermediate reasoning generated by MLLMs-T. Stage III synthesizes insights regarding reasoning strategies, effectiveness, and common failure patterns across different tasks and models.

correctness and reasoning fidelity, offering new evaluation directions for future multi-modal model architecture.

2 MMMR: Benchmarking Massive Multi-Modal Reasoning Tasks

The **MMLU-Reason** is a challenging benchmark dataset meticulously crafted to evaluate the reasoning capabilities of Multi-modal Large Language Models with intermediate Thinking (MLLMs-T). Unlike previous benchmarks [7, 16, 19, 33] which predominantly measure perception or general knowledge, **MMLU-Reason** emphasizes complex reasoning tasks requiring deep integration across diverse modalities, such as text, images, and structured data. Motivated by recent advancements in MLLMs-T, exemplified by Gemini-2.5 Pro [12], which leverage intermediate reasoning processes to enhance performance, we propose a rigorous three-stage evaluation pipeline. This pipeline is specifically designed to evaluate multi-modal reasoning quality and, crucially, assess the effectiveness and robustness of intermediate thinking. As illustrated in Figure 2, our evaluation pipeline comprises three core stages: (I) Reasoning Dataset Construction, (II) Thinking Quality Assessment, and (III) Reasoning Insights Synthesis.

2.1 Stage I: Reasoning Dataset Construction

In this initial stage, we construct the **MMLU-Reason** dataset to thoroughly evaluate MLLMs-T across a wide spectrum of reasoning scenarios. The **MMLU-Reason** comprises 1,083 carefully curated multi-modal tasks, systematically categorized into six distinct reasoning types: Logic (16.8%), Math (19.5%), Space-Time (18.5%), Code (13.0%), Map (13.8%), and Science (18.3%). Each reasoning type further includes task-specific subcategories, such as deductive inference, algebraic calculation, temporal ordering, code generation, spatial planning, and hypothesis evaluation. The **MMLU-Reason** incorporates heterogeneous modalities including natural language texts, visual imagery, and structured data (e.g., Three-View diagrams, Plots & Charts, and Web Pages). To facilitate reproducible and granular evaluation, the dataset is partitioned into a validation set (106 samples) and a test set (977 samples).

2.2 Stage II: Thinking Quality Assessment

This stage systematically evaluates the quality and structure of intermediate reasoning processes (i.e., *thinking*) produced by MLLMs-T. We propose a reasoning trace evaluation pipeline (RTEP),

including metrics: 1) RTQ, quantifying the relevance of *thinking* with the posed question, and 2) RTA, assessing logical relevance between *thinking* and the answer. Both metrics are normalized within the [0,1] interval and evaluated through standardized prompts designed for precise, unbiased assessment. Furthermore, we conduct an extensive error type analysis, categorizing reasoning failures into distinct types, including thinking errors and answer errors. This fine-grained analysis offers critical insights into the strengths and vulnerabilities inherent in the reasoning approaches adopted by MLLMs-T.

2.3 Stage III: Reasoning Insights Synthesis

The final stage synthesizes the observations from Stage II to generate holistic reasoning insights. We pursue three primary analytical objectives: 1) comparing and benchmarking the performance of MLLMs-T against standard MLLMs across different reasoning tasks, 2) profiling the quality of intermediate reasoning to identify consistent patterns of strength and weakness, and 3) investigating how prevalent error types (especially overthinking and redundant reasoning stages) impact the overall reliability of reasoning outcomes. By aggregating and analyzing detailed results across various tasks and model variants, this stage supports informed interpretation of reasoning behavior.

2.4 Research Questions

To systematically guide our evaluation and produce insightful analyses on the reasoning capabilities of MLLMs-T, we articulate the following research questions:

- [RQ1] How do MLLMs-T perform in comparison to standard MLLMs concerning reasoning accuracy across the diverse and challenging multi-modal tasks presented in **MMLU-Reason**?
- [RQ2] How does the quality of intermediate thinking generated by MLLMs-T vary across different levels of task complexity and modality combinations?
- [RQ3] Which reasoning error types are most frequently encountered by MLLMs-T within different task contexts of **MMLU-Reason**, and how do these errors reflect underlying challenges in multi-modal integration?

3 Experiment Settings

Multi-Modal Language Models without Thinking (MLLMs). MLLMs solve multi-modal tasks by directly mapping perception inputs to answers, bypassing explicit reasoning steps. We evaluate representative models from both open-source and closed-source. Open-source MLLMs include LLaVA-3.2-11B-Vision-Instruct [25], LLaVA-3.2-90B-Vision-Instruct [25], Qwen2.5-VL-32B-Instruct [2], Qwen2.5-VL-72B-Instruct [3], and Qwen-VL-max [1]. Closed-source MLLMs include Gemini-1.5 Flash [10], GPT-4 Vision [35], and LLaMA-4-Maverick [4], recognized for their sophisticated multi-modal fusion and retrieval-based response capabilities.

Multi-Modal Language Models with Thinking (MLLMs-T). MLLMs-T extend the capabilities of MLLMs by producing intermediate reasoning traces before final answer generation. This architecture allows structured, step-wise reasoning and facilitates deeper interpretability in complex problem-solving. We include open models such as QVQ-72B-Preview [5], and several advanced proprietary models, including Gemini-2.0 Flash [11], Gemini-2.5 Pro [13], Claude-3.7-sonnet [6], and o4-mini [36]. A particularly notable configuration is our custom *Dual Model*, which simulates MLLMs-T behavior by integrating the strengths of two distinct models. Specifically,

Table 1: Comparison of representative multi-modal reasoning datasets. **V** (Visual Input), **OC** (Optical Characters), **I+T** (Image + Text), **IL** (Interleaved Format), **TJ** (Thinking Judgment) and **Source** (W: Web, T: Textbook, R: Remake).

Dataset	Size	Images	Format	Source	Reason	TJ
VQA [7]	>1M	V	I+T	W	Low	⊗
GQA [16]	>1M	V	I+T	R	Medium	⊗
VizWiz [9]	32K	V	I+T	W	Low	⊗
TextVQA [40]	45K	OC	I+T	W	Medium	⊗
OK-VQA [34]	14K	V+OC	I+T	W	Medium	⊗
SEED [23]	19K	V+OC	I+T	W	Medium	⊗
MMBench [30]	3K	V+OC	I+T	W+R	Medium	⊗
MM-Vet [46]	0.2K	V+OC	I+T	W	Medium	⊗
ScienceQA [32]	6K	5 Types	I+T	T	Medium	⊗
MME-COT [18]	1.1K	-	IL	W+R	Medium	⊗
EMMA [15]	2.7K	-	IL	W+R	Medium	⊗
MMMU [47]	11.5K	30 Types	IL	W+T	Medium	⊗
MMLU-Reason	1.1K	15 Types	IL	W+T+R	High	✓

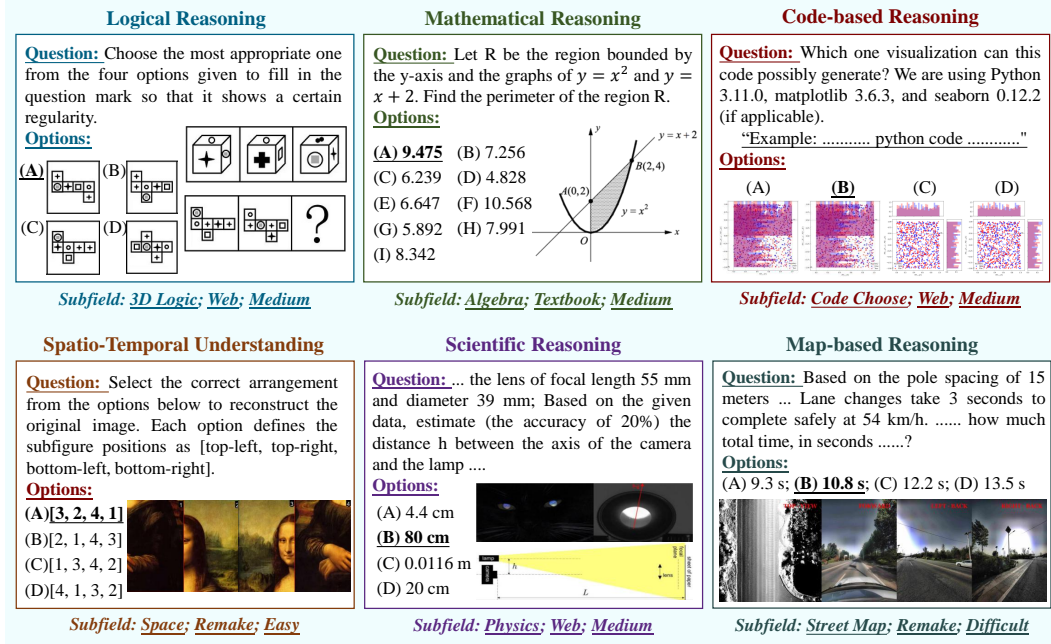


Figure 3: Representative multi-modal reasoning samples from **MMLU-Reason**. Each example consists of interleaved image-text input, a complex reasoning question, annotation, and source information. The samples illustrate the dataset’s high structural variability and reasoning depth.

GPT-4V [35] is responsible for parsing the input question and image content—handling rich visual understanding and language grounding. The parsed task is then passed to DeepSeek-R1 [14] for structured multi-step reasoning. This pipeline allows us to isolate and examine the effect of high-quality Thinking traces independently of perception noise. Moreover, since DeepSeek-R1 is optimized for textual reasoning rather than vision, this dual formulation ensures modular design and enhanced control over each reasoning stage.

Datasets. The **MMLU-Reason** is designed from first principles to meet the demands of benchmarking multi-modal reasoning with Thinking. Compared to prior works like MMMU [47], MME-CoT [18], and EMMA [15], **MMLU-Reason** provides a full-spectrum redesign of reasoning task settings. Each of its 1,083 problems is carefully constructed and categorized into six reasoning types and sixteen fine-grained subfields, providing targeted coverage of logical, mathematical, spatio-temporal, code, map-based, and scientific reasoning. The dataset incorporates a rich array of visual stimuli, including charts, diagrams, 3D maps, and visual code logic, covering 15 unique image types. Unlike retrieval-centric tasks, many questions require long-horizon reasoning, abstraction, or visual-spatial synthesis. To further increase complexity, 44.6% of the items are remade or enhanced beyond web or textbook sources. Moreover, **MMLU-Reason** facilitates intermediate reasoning evaluation. For each sample, the source origin (Web, Textbook, Remake), and task type are documented, supporting both output-based and process-based analysis. This structure enables deep introspection into where and how reasoning fails or succeeds, making it a unique testbed for evaluating MLLMs-T.

Table 2: Statistics of **MMLU-Reason**, detailing the distribution and characteristics of six tasks.

Category	Value
Quantitative statistics	
Total Questions	1083
Total Subjects/Subfields	6/16
Image Types	15
Dataset Split	
Validation:Test	106:977
Difficulties (Easy:Medium:Hard)	30%:40%:30%
Task Type Distribution	
Logical Reasoning	182 (16.8%)
Mathematical Reasoning	212 (19.5%)
Spatio-Temporal Understanding	200 (18.5%)
Code Reasoning	141 (13.0%)
Map Reasoning	150 (13.8%)
Science Reasoning	198 (18.4%)
Content Characteristics	
Average Question Length	68.75 words
Average Option Length	12.25 words
Average Response Length	135.60 words
Multi-modal Inputs per Question	1.85
Reasoning Steps per Question	3.42
Annotation and Complexity	
Remade Questions	483 (44.6%)
Average Reasoning Depth	4.15 levels
Cross-Modal Integration Rate	95.2%

Table 3: Accuracy (%) comparison of baselines, MLLMs, and MLLMs-T on the **MMLU-Reason**. Each row highlights the per-model highest and lowest scores using green and red, respectively. For each column (task type), the best-performing model is indicated in **bold** and the second-best is underline. Models marked with * are closed-source. “S-T” denotes the Space-Time.

	Validation (106)	Test (977)	Logic (182)	Math (212)	S-T (200)	Code (141)	Map (150)	Science (198)
Baselines								
Random Choice	22.1	23.62	24.18	24.06	21.50	25.53	22.67	23.74
Frequent Choice	26.8	26.58	26.92	26.42	24.00	24.82	25.33	29.80
Expert (Human only)	29.23	-	-	-	-	-	-	-
Expert (Human + GPT-4o [17])	52.85	-	-	-	-	-	-	-
Multi-Modal Large Language Models without Thinking								
LLaVA-3.2-11B-Vision-Instruct [25]	24.53	23.92	18.68	31.13	28.00	13.48	22.67	22.73
LLaVA-3.2-90B-Vision-Instruct [25]	30.19	27.65	21.43	34.91	35.00	17.73	25.33	21.72
Qwen2.5-VL-32B-Instruct [2]	34.86	34.90	25.27	45.28	45.00	32.62	36.67	21.72
Qwen2.5-VL-72B-Instruct [3]	36.95	37.18	24.18	46.70	47.50	41.84	42.67	31.31
Qwen-VL-max [1]	35.13	35.55	24.18	47.17	46.00	39.01	35.33	28.28
Gemma-3-27B-IT [41]	30.87	29.01	22.53	42.45	33.50	34.75	26.67	27.27
Gemini-1.5 Flash* [10]	32.18	29.61	28.57	37.74	37.00	18.44	24.67	32.83
GPT-4 Vision* [35]	37.59	38.05	28.02	35.85	49.00	28.37	32.00	41.92
LLaMA-4-Maverick* [4]	40.68	<u>41.82</u>	30.77	44.81	46.00	<u>37.59</u>	30.67	38.38
Multi-Modal Large Language Models with Thinking								
QVQ-72B-Preview [5]	30.94	32.09	26.37	38.21	42.00	32.62	31.33	32.83
Gemini-2.0 Flash* [11]	37.63	37.89	35.16	50.47	49.50	28.37	30.67	41.41
Gemini-2.5 Pro* [13]	42.45	42.36	39.56	41.51	44.50	36.17	37.33	46.46
Claude-3.7-sonnet* [6]	38.28	37.72	<u>35.71</u>	45.75	51.00	21.28	34.00	43.94
o4-mini* [36]	38.64	37.58	34.62	46.23	47.50	19.86	29.33	41.41
Dual ([35] + DeepSeek-R1 [14])	<u>41.26</u>	41.00	<u>35.71</u>	<u>47.64</u>	48.00	22.70	22.67	<u>45.45</u>

Metrics. We evaluate MLLMs-T and MLLMs on the **MMLU-Reason** using a concise suite of metrics, with scores normalized to [0, 1]: 1) ACC, the proportion of correct answers; 2) RTQ, assessing how well the Thinking process aligns with the problem’s requirements, independent of answer correctness; 3) RTA, evaluating the logical consistency between the thinking process and the final answer, regardless of accuracy; 4) Reasoning Step Consistency (RSC), measuring logical coherence across Thinking steps through consistency checks.

4 Empirical Results and Analysis

4.1 Main Results

We evaluate 17 models on the **MMLU-Reason**, where baselines include *Random Choice* and *Frequent Choice*, which serve as naïve heuristics, and two *Expert* configurations that represent human upper bounds with or without model assistance (see Appendix A for full descriptions). As shown in Table 3, MLLMs-T overall outperform MLLMs across six tasks, highlighting the advantage of incorporating explicit thinking mechanisms. Notably, *Gemini-2.5 Pro* achieves the highest overall test accuracy at 42.36%, while the *Expert (Human + GPT-4o)* attains an upper-bound of 52.85%, indicating a remaining gap between state-of-the-art MLLMs-T and human-assisted reasoning [RQ1 Summary].

Model-wise performance reflects generalization differences. By examining the best and second-best performers for each task column, we observe that *Gemini-2.5 Pro* (with 4 best and 1 second-best scores) exhibits the most stable and competitive accuracy across reasoning types. This suggests that explicit reasoning modules, when paired with carefully supervised thinking strategies, enable strong generalization across diverse task formats. *Gemini-2.0 Flash* performs robustly in Math (50.47%) but shows a significant drop in Code, indicating limited cross-domain transferability. The *Dual* achieves strong results in Logic and Science, supporting the effectiveness of modular architectural design. In contrast, open-source models like *Qwen2.5-VL-72B* and *Qwen-VL-max* display isolated strengths in domains such as Spatio-Temporal reasoning and Code, but lack consistency. Weaker models (e.g., *Gemma-3-27B* and *LLaVA-3.2-11B*) show broad performance variance and struggle particularly with symbolically dense or spatial tasks, indicating limitations in reasoning depth despite model size.

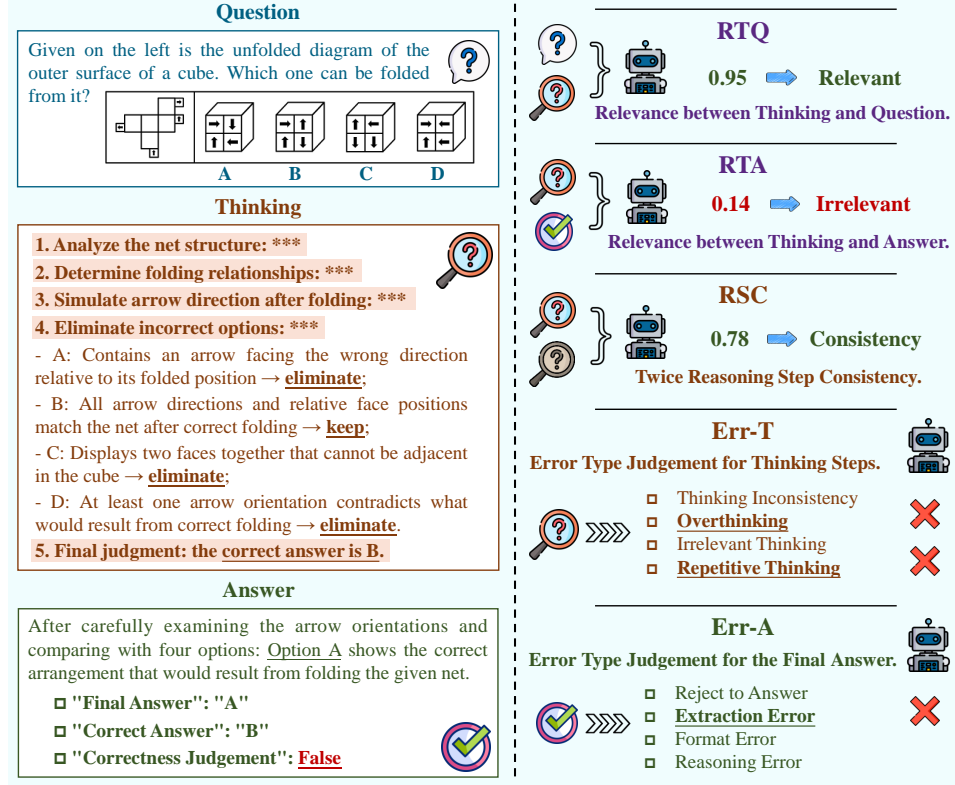


Figure 4: Overview of the Reasoning Trace Evaluation Pipeline (RTEP). The pipeline applies structured scoring of intermediate reasoning traces, evaluating consistency, relevance, and verbosity.

Task-wise analysis reveals variation in reasoning difficulty. A row-wise comparison of model accuracy extremes reveals task-dependent performance variability. *Math* and *Space-Time* tasks, which dominate the best-performing entries (green highlights), are generally more tractable, suggesting progress in symbolic computation and spatial comprehension. In contrast, tasks like *Logic* and especially *Code* show lower accuracy ceilings (often below 42%) and greater inter-model dispersion, as evidenced by the concentration of minimum scores (red highlights). These patterns underscore the utility of **MMLU-Reason** in enabling fine-grained analysis of multimodal reasoning capabilities, offering a more diagnostic lens than aggregate performance alone.

4.2 Thinking Quality Analysis

To evaluate intermediate reasoning quality beyond answer correctness, we introduce the Reasoning Trace Evaluation Pipeline (RTEP). This structured pipeline annotates and scores each model’s reasoning trace across three dimensions: Relevance to the Question (RTQ), Relevance to the Answer (RTA), and Reasoning Step Consistency (RSC), each rated on a 0–10 scale. Leveraging GPT-4o [17] as an automated evaluator, RTEP enables scalable, semantically aligned trace assessments, avoiding the subjectivity and cost of manual annotation. As illustrated in Figure 4, this design allows for model-agnostic diagnosis of coherence, verbosity, and reasoning alignment, enabling targeted comparisons across architectures and task types.

Table 4 summarizes a detailed comparison between Claude-3.7-sonnet and Dual (GPT-4V + DeepSeek-R1) across all six reasoning tasks in **MMLU-Reason**. Claude-3.7 consistently outperforms Dual in Overall Score (OS), with especially strong results in Math and Science, where compact, logically consistent traces are essential. In contrast, the Dual system achieves marginally higher answer accuracy in several tasks (e.g., Logic: +2.79%), but at the cost of reasoning coherence, as reflected in lower OS values and significantly inflated trace lengths (TLen often 3–5× higher). This indicates that longer outputs, while occasionally improving accuracy, tend to dilute reasoning relevance and introduce redundancy or inconsistency. For instance, in Code and Space-Time tasks, Dual’s modular pipeline leads to repetitive or loosely linked steps, revealing that increased trace

Table 4: Comparison of reasoning quality between Claude-3.7-sonnet and Dual across six task types. RTQ, RTA, RSC are reasoning trace metrics in [0–10]; ACC is final answer accuracy (%); OS is a weighted overall score ($0.3 \cdot RTQ + 0.3 \cdot RTA + 0.3 \cdot RSC + 0.1 \cdot (ACC \times 0.1)$); TLen denotes trace length in thousands of tokens; ThinkErr indicates dominant reasoning flaw (defined in Section 4.3).

Task	Model	RTQ	RTA	RSC	ACC (%)	OS	TLen (k)	ThinkErr
Logic	Claude-3.7-sonnet	9.39	9.41	9.07	35.71	8.72	3.71	Overthinking
	Dual	6.32	7.63	6.18	38.50	6.42	15.19	Irrelevant Thinking
	Δ (Dual–Claude)	-	-	-	+ 2.79	- 2.30	+ 11.48	-
Math	Claude-3.7-sonnet	8.88	9.02	8.40	45.75	8.35	5.32	Overthinking
	Dual	8.57	8.80	7.82	47.60	8.03	21.35	Overthinking
	Δ (Dual–Claude)	-	-	-	+ 1.85	- 0.32	+ 16.03	-
Space-Time	Claude-3.7-sonnet	9.50	9.26	8.97	51.00	8.83	2.38	Overthinking
	Dual	8.50	8.75	7.60	48.00	8.32	14.83	Repetitive Thinking
	Δ (Dual–Claude)	-	-	-	- 3.00	- 0.51	+ 12.45	-
Code	Claude-3.7-sonnet	9.56	9.31	9.30	21.28	8.82	4.53	Repetitive Thinking
	Dual	8.61	8.56	7.94	22.90	7.93	17.24	Inconsistency
	Δ (Dual–Claude)	-	-	-	+ 1.62	- 0.89	+ 12.71	-
Map	Claude-3.7-sonnet	9.17	8.94	8.43	23.80	8.57	1.76	Irrelevant Thinking
	Dual	7.08	7.42	6.42	22.50	6.99	12.43	Repetitive Thinking
	Δ (Dual–Claude)	-	-	-	- 1.30	- 1.58	+ 10.67	-
Science	Claude-3.7-sonnet	8.95	9.29	8.73	43.93	8.77	3.61	Inconsistency
	Dual	8.25	8.84	7.81	45.10	8.32	14.50	Inconsistency
	Δ (Dual–Claude)	-	-	-	+ 1.17	- 0.45	+ 10.89	-

length does not ensure better reasoning quality. These findings emphasize that answer correctness alone is insufficient as a proxy for reasoning performance—models with higher accuracy can still produce flawed, verbose, or semantically incoherent rationales. Evaluating trace quality is thus essential for advancing the robustness and interpretability of MLLMs-T.

Overall, accurate answers do not guarantee sound reasoning. Our findings reveal that high-performing MLLMs-T can still produce incoherent thought processes, suggesting that future progress hinges not only on output correctness but on the quality of the reasoning path itself [RQ2 Summary].

4.3 Thinking and Answer Error Types Analysis

To understand the structural weaknesses in multimodal reasoning, we analyze errors in both intermediate *Thinking* traces and final *Answer* predictions of Claude-3.7-sonnet on the **MMLU-Reason** validation set. As visualized in Figure 5, we classify each error into semantically distinct categories, allowing targeted diagnosis of reasoning failures.

Thinking Errors Distribution.

- 1) *Inconsistency* (41.5%) reflects internal contradictions or self-conflicting logic, often arising in Science or Logic tasks where maintaining state across steps is nontrivial.
- 2) *Overthinking* (20.5%) denotes unnecessarily verbose or speculative reasoning paths. These are prevalent in otherwise simple tasks where compact reasoning suffices.
- 3) *Irrelevant Thinking* (18.5%) includes content unrelated to the question or answer. These errors typically occur in poorly grounded inputs or under weak alignment.
- 4) *Repetitive Thinking* (16.2%) captures duplication without informational gain, frequently observed in Code and Map, where step-tracking or termination is difficult.
- 5) *Others* (3.8%) contain rare phenomena such as speculative completion or omitted critical steps.

Answer Errors Distribution.

- 1) *Reasoning Error* (43.6%) indicates logically flawed reasoning that nonetheless produces confident but incorrect answers, especially common in Math and Science.
- 2) *Perceptual Error* (28.2%) reflects misinterpretation of visual data such as spatial layouts or charts—frequent in Map and Space-Time tasks.
- 3) *Format Error* (9.4%) denotes violations of expected output formats, such as missing labels or extraneous text, often due to instruction-following deficiencies.

4) *Answer Extraction Error* (7.1%) occurs when models generate lengthy thinking traces but omit or fail to commit to a final answer—highlighting uncertainty or incomplete reasoning convergence.

5) *Reject to Answer* (4.7%) involves abstention despite solvable inputs, typically due to cautious decoding or alignment penalties.

6) *Others* (7.0%) include ambiguous completions or partially correct statements.

Error Analysis. The error distributions suggest that high answer accuracy often masks underlying reasoning path defects. The dominance of inconsistency and overthinking in reasoning traces reveals fundamental challenges in maintaining logical control and brevity. Likewise, the prevalence of reasoning-based answer errors over perceptual ones underscores that symbolic structure, rather than visual understanding, remains the primary bottleneck in high-level multimodal cognition. These findings reinforce the importance of trace-aware evaluation: coarse answer-level metrics alone cannot capture reasoning fidelity [RQ3 Summary].

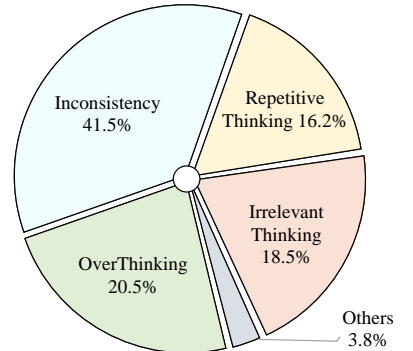
5 Related Work

Multi-Modal Large Language Models Benchmarking. The evaluation of multimodal reasoning has progressed from VQAv2 [7], GQA [16], and VCR [48] to broader and more specialized datasets such as TextVQA [40], ScienceQA [32], AI2D [20], and SEED [23], and recent large-scale benchmarks like MM-Bench [30], MM-Vet [46], EMMA [15], MathVista [31], and MMMU [47]. These datasets have advanced task diversity and domain specificity, yet most focus primarily on answer accuracy with limited insight into reasoning quality. While efforts such as MME-CoT [18] introduce reasoning trace annotations, they mainly rely on additional CoT designs. In contrast, our **MMLU-Reason** is constructed as a high-difficulty, multi-domain dataset specifically for evaluating multimodal reasoning. It not only spans six distinct reasoning types with structured task design but also supports fine-grained assessment of thinking in MLLMs-T, offering a comprehensive diagnostic standard for future multimodal models.

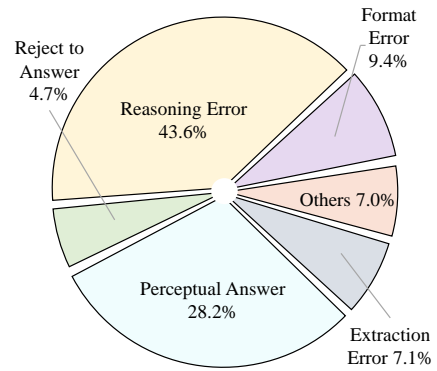
Reasoning Traces and Thinking Evaluation. In textual LLMs, reasoning trace prompting methods like Chain-of-Thought [42], ReAct [45], and Reflexion [39] have improved interpretability and performance through explicit step-by-step reasoning. Recent works propose evaluation tools such as RATER [27] and DECKARD [26] to assess coherence, faithfulness, and hallucination in these traces. However, such evaluations are still limited to language-only settings. Our work fills this gap by enabling trace-level reasoning evaluation within a multimodal benchmark, supporting both process- and outcome-oriented assessments.

6 Conclusion

This paper presents **MMLU-Reason**, a new benchmark and evaluation framework for advancing the study of multi-modal reasoning in large language models. Distinct from prior efforts that primarily emphasize perception or answer correctness, **MMLU-Reason** targets high-complexity, symbolic reasoning across six diverse domains, including logic, mathematics, and space-time inference. To systematically assess reasoning fidelity, we propose the Reasoning Trace Evaluation Pipeline (RTEP), which incorporates structured metrics (RTQ, RTA, RSC), length-efficiency analysis, and error-type classification to evaluate the coherence and relevance of intermediate thinking. Through extensive experiments on 17 models, we find that MLLMs-T overall outperform standard MLLMs in tasks



a) Thinking Error Distribution



b) Answer Error Distribution

Figure 5: Distribution of Thinking and Answer Errors on Claude-3.7-sonnet.

requiring structured reasoning. Our findings suggest that improving multi-modal reasoning requires not just stronger instruction tuning or scale, but more cognitively aligned architectures that optimize for both answer correctness and thinking quality. We hope this benchmark catalyzes further research on reflective reasoning, modular cognition, and generalizable multi-modal understanding.

Limitations. While **MMLU-Reason** emphasizes reasoning difficulty and multi-modal integration, it does not explicitly define fine-grained difficulty levels or hierarchical task groupings. This limits the granularity of comparative analysis across reasoning complexity levels. The main challenge lies in accurately quantifying reasoning difficulty across diverse modalities and task structures, which requires both task-specific cognitive modeling and robust annotation protocols. Future work should explore dynamic task stratification to better support curriculum learning, diagnostic evaluation, and model scalability studies.

References

- [1] Alibaba DAMO Academy. Qwen-vl-max: Most capable visual-language model. <https://github.com/QwenLM/Qwen-VL>, 2024. Accessed: 2025-05-14.
- [2] Alibaba DAMO Academy. Qwen2.5-vl-32b-instruct: Vision-language model. <https://huggingface.co/Qwen/Qwen2.5-VL-32B-Instruct>, 2025. Accessed: 2025-05-14.
- [3] Alibaba DAMO Academy. Qwen2.5-vl-72b-instruct: Vision-language model. <https://huggingface.co/Qwen/Qwen2.5-VL-72B-Instruct>, 2025. Accessed: 2025-05-14.
- [4] Meta AI. Llama 4 maverick: Natively multimodal model. <https://ai.meta.com/blog/llama-4-multimodal-intelligence/>, 2025. Accessed: 2025-05-14.
- [5] Qwen AI. Qvq-72b-preview: Vision-language model. <https://huggingface.co/Qwen/QVQ-72B-Preview>, 2025. Accessed: 2025-05-14.
- [6] Anthropic. Claude 3.7 sonnet: Multimodal model. <https://www.anthropic.com/clause-3-7-sonnet>, 2025. Accessed: 2025-05-14.
- [7] Stanislaw Antol, Aishwarya Agrawal, Jiasen Lu, Margaret Mitchell, Dhruv Batra, C Lawrence Zitnick, and Devi Parikh. Vqa: Visual question answering. In *Proceedings of the IEEE international conference on computer vision*, pages 2425–2433, 2015.
- [8] Jinze Bai, Shuai Bai, Shusheng Yang, Shijie Wang, Sinan Tan, Peng Wang, Junyang Lin, Chang Zhou, and Jingren Zhou. Qwen-vl: A versatile vision-language model for understanding, localization, text reading, and beyond. *arXiv preprint arXiv:2308.12966*, 2023.
- [9] Jeffrey P. Bigham, Chandrika Jayant, Hanjie Ji, Greg Little, Andrew Miller, Robert C. Miller, Robin Miller, Aubrey Tatarowicz, Brandy White, Samuel White, and Tom Yeh. Vizwiz: Nearly real-time answers to visual questions. In *Proceedings of the 23rd Annual ACM Symposium on User Interface Software and Technology (UIST)*, pages 333–342. ACM, 2010.
- [10] Google DeepMind. Gemini 1.5 flash: Multimodal model. <https://cloud.google.com/vertex-ai/generative-ai/docs/models/gemini/1-5-flash>, 2024. Accessed: 2025-05-14.
- [11] Google DeepMind. Gemini 2.0 flash: Multimodal model. <https://cloud.google.com/vertex-ai/generative-ai/docs/models/gemini/2-0-flash>, 2024. Accessed: 2025-05-14.
- [12] Google DeepMind. Gemini 2.5: Our most intelligent ai model. <https://blog.google/technology/google-deepmind/gemini-model-thinking-updates-march-2025/>, 2025. Accessed: 2025-05-14.
- [13] Google DeepMind. Gemini 2.5 pro: Multimodal model. <https://cloud.google.com/vertex-ai/generative-ai/docs/models/gemini/2-5-pro>, 2025. Accessed: 2025-05-14.
- [14] Daya Guo, Dejian Yang, Haowei Zhang, Junxiao Song, et al. Deepseek-r1: Incentivizing reasoning capability in llms via reinforcement learning. <https://arxiv.org/abs/2501.12948>, 2025. Accessed: 2025-05-14.

[15] Yunzhuo Hao, Jiawei Gu, Huichen Will Wang, Linjie Li, Zhengyuan Yang, Lijuan Wang, and Yu Cheng. Can mllms reason in multimodality? emma: An enhanced multimodal reasoning benchmark. <https://arxiv.org/abs/2501.05444>, 2025. Accessed: 2025-05-14.

[16] Drew A Hudson and Christopher D Manning. Gqa: A new dataset for real-world visual reasoning and compositional question answering. In *Proceedings of the IEEE Conference on Computer Vision and Pattern Recognition*, pages 6700–6709, 2019.

[17] Aaron Hurst, Adam Lerer, Adam P Goucher, Adam Perelman, Aditya Ramesh, Aidan Clark, AJ Ostrow, Akila Welihinda, Alan Hayes, Alec Radford, et al. Gpt-4o system card. *arXiv preprint arXiv:2410.21276*, 2024.

[18] Dongzhi Jiang, Renrui Zhang, Ziyu Guo, Yanwei Li, Yu Qi, Xinyan Chen, Liuhi Wang, Jianhan Jin, Claire Guo, Shen Yan, Bo Zhang, Chaoyou Fu, Peng Gao, and Hongsheng Li. Mme-cot: Benchmarking chain-of-thought in large multimodal models for reasoning quality, robustness, and efficiency. <https://arxiv.org/abs/2502.09621>, 2025. Accessed: 2025-05-14.

[19] Justin Johnson, Bharath Hariharan, Laurens van der Maaten, Li Fei-Fei, C Lawrence Zitnick, and Ross Girshick. Clevr: A diagnostic dataset for compositional language and elementary visual reasoning. In *Proceedings of the IEEE conference on computer vision and pattern recognition*, pages 2901–2910, 2017.

[20] Aniruddha Kembhavi, M. Salvato, M. Seo, H. Hajishirzi, and A. Farhadi. A diagram is worth a dozen images. In *Proceedings of the European Conference on Computer Vision (ECCV)*, pages 235–251, 2016.

[21] Kaixin Li, Yuchen Tian, Qisheng Hu, Ziyang Luo, Zhiyong Huang, and Jing Ma. Mmcode: Benchmarking multimodal large language models for code generation with visually rich programming problems. *arXiv preprint arXiv:2404.09486*, 2024.

[22] Kaixin Li, Yuchen Tian, Qisheng Hu, Ziyang Luo, Zhiyong Huang, and Jing Ma. Web2code: Benchmarking multimodal large language models for code generation with visually rich programming problems. *Findings of the Association for Computational Linguistics: EMNLP 2024*, pages 736–783, 2024.

[23] Yixuan Li, Yujie Wang, Yujie Zhang, Yifan Wang, Yujie Wang, Yixuan Li, Yujie Wang, Yujie Zhang, and Yifan Wang. Seed-bench: Benchmarking multimodal large language models. In *Proceedings of the IEEE/CVF Conference on Computer Vision and Pattern Recognition (CVPR)*, 2024.

[24] Haotian Liu, Chunyuan Li, Qingyang Wu, and Yong Jae Lee. Visual instruction tuning. *arXiv preprint arXiv:2304.08485*, 2023.

[25] Haotian Liu, Chunyuan Li, Qingyang Wu, and Yong Jae Lee. Visual instruction tuning. <https://arxiv.org/abs/2304.08485>, 2023. Accessed: 2025-05-14.

[26] Jiacheng Liu, Pan Lu, Hritik Bansal, Hannaneh Hajishirzi, and Jianfeng Gao. Deckard: Benchmarking reasoning traces in language models. In *Proceedings of the 2023 Conference on Empirical Methods in Natural Language Processing*, 2023.

[27] Jiacheng Liu, Pan Lu, Hritik Bansal, Hannaneh Hajishirzi, and Jianfeng Gao. Rater: Reference-free evaluation for cot reasoning. In *Proceedings of the 2023 Conference on Empirical Methods in Natural Language Processing*, 2023.

[28] Yibo Liu et al. Mapeval-visual: A benchmark for visual map-based planning tasks. *arXiv preprint arXiv:2405.67890*, 2024.

[29] Yibo Liu et al. Multi-modal-self-instruct: Synthesizing complex visual reasoning context using language models. *arXiv preprint arXiv:2405.12345*, 2024.

[30] Yuxin Liu, Yuxuan Zhang, Yifan Wang, Yixuan Li, Yujie Wang, Yujie Zhang, and Yifan Wang. Mmbench: Is your multi-modal model an all-around player? *arXiv preprint arXiv:2307.06281*, 2023.

[31] Pan Lu, Hritik Bansal, Tony Xia, Jiacheng Liu, Chunyuan Li, Hannaneh Hajishirzi, Hao Cheng, Kai-Wei Chang, Michel Galley, and Jianfeng Gao. Mathvista: Evaluating mathematical reasoning of foundation models in visual contexts. In *Proceedings of the International Conference on Learning Representations (ICLR)*, 2024.

[32] Pan Lu, Swaroop Mishra, Tony Xia, Liang Qiu, Kai-Wei Chang, Song-Chun Zhu, Oyvind Tafjord, Peter Clark, and Ashwin Kalyan. Learn to explain: Multimodal reasoning via thought chains for science question answering. In *Advances in Neural Information Processing Systems (NeurIPS)*, 2022.

[33] Pan Lu, Xiang Wang, Zehao Lin, Zekun Zhang, Mo Yu, Zhiyuan Yu, et al. Learn from peers: Equipping multi-modal learners with cross-modal memory. In *Advances in Neural Information Processing Systems (NeurIPS)*, 2022.

[34] Kenneth Marino, Mohammad Rastegari, Ali Farhadi, and Hannaneh Hajishirzi. Ok-vqa: A visual question answering benchmark requiring external knowledge. In *Proceedings of the IEEE/CVF Conference on Computer Vision and Pattern Recognition (CVPR)*, pages 3195–3204, 2019.

[35] OpenAI. Gpt-4 vision: Multimodal model. <https://openai.com/index/gpt-4v-system-card/>, 2023. Accessed: 2025-05-14.

[36] OpenAI. o4-mini: Multimodal model. <https://openai.com/o4-mini>, 2025. Accessed: 2025-05-14.

[37] Alec Radford, Jong Wook Kim, Chris Hallacy, Aditya Ramesh, Gabriel Goh, Sandhini Agarwal, Girish Sastry, Amanda Askell, Pamela Mishkin, Jack Clark, Scott Krueger, and Ilya Sutskever. Learning transferable visual models from natural language supervision. In *Proceedings of the International Conference on Machine Learning (ICML)*, pages 8748–8763, 2021.

[38] Piyush Sharma, Nan Ding, Sebastian Goodman, and Radu Soricut. Conceptual captions: A cleaned, hypernymed, image alt-text dataset for automatic image captioning. In *Proceedings of the 56th Annual Meeting of the Association for Computational Linguistics (Volume 1: Long Papers)*, pages 2556–2565, 2018.

[39] Noah Shinn, Federico Cassano, Edward Berman, Ashwin Gopinath, and Karthik Narasimhan. Reflexion: Language agents with verbal reinforcement learning. In *Proceedings of the 2023 Conference on Empirical Methods in Natural Language Processing*, 2023.

[40] Amanpreet Singh, Vivek Natarajan, Xinlei Jiang, Xi Chen, Marcus Rohrbach, Dhruv Batra, and Devi Parikh. Towards vqa models that can read. In *Proceedings of the IEEE/CVF Conference on Computer Vision and Pattern Recognition (CVPR)*, pages 8317–8326, 2019.

[41] Gemma Team, Aishwarya Kamath, Johan Ferret, Shreya Pathak, Nino Vieillard, Ramona Merhej, Sarah Perrin, Tatiana Matejovicova, Alexandre Ramé, Morgane Rivière, Louis Rouillard, Thomas Mesnard, Geoffrey Cideron, Jean-Bastien Grill, Sabela Ramos, Edouard Yvinec, Michelle Casbon, Etienne Pot, Ivo Penchev, Gaël Liu, Francesco Visin, Kathleen Kenealy, Lucas Beyer, Xiaohai Zhai, Anton Tsitsulin, Robert Busa-Fekete, Alex Feng, Noveen Sachdeva, Benjamin Coleman, Yi Gao, Basil Mustafa, Iain Barr, Emilio Parisotto, David Tian, Matan Eyal, Colin Cherry, Jan-Thorsten Peter, Danila Sinopalnikov, Surya Bhupatiraju, Rishabh Agarwal, Mehran Kazemi, Dan Malkin, Ravin Kumar, David Vilar, Idan Brusilovsky, Jiaming Luo, Andreas Steiner, Abe Friesen, Abhanshu Sharma, Abheesht Sharma, Adi Mayrav Gilady, Adrian Goedeckemeyer, Alaa Saade, Alex Feng, Alexander Kolesnikov, Alexei Bendebury, Alvin Abdagic, Amit Vadi, András György, André Susano Pinto, Anil Das, Ankur Bapna, Antoine Miech, Antoine Yang, Antonia Paterson, Ashish Shenoy, Ayan Chakrabarti, Bilal Piot, Bo Wu, Bobak Shahriari, Bryce Petrini, Charlie Chen, Charline Le Lan, Christopher A. Choquette-Choo, CJ Carey, Cormac Brick, Daniel Deutsch, Danielle Eisenbud, Dee Cattle, Derek Cheng, Dimitris Paparas, Divyashree Shivakumar Sreepathihalli, Doug Reid, Dustin Tran, Dustin Zelle, Eric Noland, Erwin Huizenga, Eugene Kharitonov, Frederick Liu, Gagik Amirkhanyan, Glenn Cameron, Hadi Hashemi, Hanna Klimczak-Plucińska, Harman Singh, Harsh Mehta, Harshal Tushar Lehri, Hussein Hazimeh, Ian Ballantyne, Idan Szpektor, Ivan Nardini, Jean Pouget-Abadie, Jetha Chan, Joe Stanton, John Wieting, Jonathan Lai, Jordi

Orbay, Joseph Fernandez, Josh Newlan, Ju yeong Ji, Jyotinder Singh, Kat Black, Kathy Yu, Kevin Hui, Kiran Vodrahalli, Klaus Greff, Linhai Qiu, Marcella Valentine, Marina Coelho, Marvin Ritter, Matt Hoffman, Matthew Watson, Mayank Chaturvedi, Michael Moynihan, Min Ma, Nabila Babar, Natasha Noy, Nathan Byrd, Nick Roy, Nikola Momchev, Nilay Chauhan, Noveen Sachdeva, Oskar Bunyan, Pankil Botarda, Paul Caron, Paul Kishan Rubenstein, Phil Culliton, Philipp Schmid, Pier Giuseppe Sessa, Pingmei Xu, Piotr Stanczyk, Pouya Tafti, Rakesh Shivanna, Renjie Wu, Renke Pan, Reza Rokni, Rob Willoughby, Rohith Vallu, Ryan Mullins, Sammy Jerome, Sara Smoot, Sertan Girgin, Shariq Iqbal, Shashir Reddy, Shruti Sheth, Siim Põder, Sijal Bhatnagar, Sindhu Raguram Panyam, Sivan Eiger, Susan Zhang, Tianqi Liu, Trevor Yacovone, Tyler Liechty, Uday Kalra, Utku Evcı, Vedant Misra, Vincent Roseberry, Vlad Feinberg, Vlad Kolesnikov, Woohyun Han, Woosuk Kwon, Xi Chen, Yinlam Chow, Yuvein Zhu, Zichuan Wei, Zoltan Egyed, Victor Cotruta, Minh Giang, Phoebe Kirk, Anand Rao, Kat Black, Nabila Babar, Jessica Lo, Erica Moreira, Luiz Gustavo Martins, Omar Sanseviero, Lucas Gonzalez, Zach Gleicher, Tris Warkentin, Vahab Mirrokni, Evan Senter, Eli Collins, Joelle Barral, Zoubin Ghahramani, Raia Hadsell, Yossi Matias, D. Sculley, Slav Petrov, Noah Fiedel, Noam Shazeer, Oriol Vinyals, Jeff Dean, Demis Hassabis, Koray Kavukcuoglu, Clement Farabet, Elena Buchatskaya, Jean-Baptiste Alayrac, Rohan Anil, Dmitry Lepikhin, Sebastian Borgeaud, Olivier Bachem, Armand Joulin, Alek Andreev, Cassidy Hardin, Robert Dadashi, and Léonard Hussenot. Gemma 3 technical report. arXiv preprint arXiv:2503.19786, 2025.

- [42] Jason Wei, Xuezhi Wang, Dale Schuurmans, Maarten Bosma, Brian Ichter, Fei Xia, Ed H. Chi, Quoc V. Le, and Denny Zhou. Chain-of-thought prompting elicits reasoning in large language models. In *Advances in Neural Information Processing Systems*, 2022.
- [43] Yijia Xiao, Edward Sun, Tianyu Liu, and Wei Wang. Logicvista: Multimodal llm logical reasoning benchmark in visual contexts. *arXiv preprint arXiv:2407.04973*, 2024.
- [44] Yunqiu Xu, Linchao Zhu, and Yi Yang. Mc-bench: A benchmark for multi-context visual grounding in the era of mllms. *arXiv preprint arXiv:2410.12332*, 2024.
- [45] Shinn Yao, Jiachang Zhao, Dian Yu, Shuyang Gao, Yujie Chen, Zhou Yu, and Karthik Narasimhan. React: Synergizing reasoning and acting in language models. In *Advances in Neural Information Processing Systems*, 2022.
- [46] Weihao Yu, Zhengyuan Yang, Lingfeng Ren, Linjie Li, Jianfeng Wang, Kevin Lin, Chung-Ching Lin, Zicheng Liu, Lijuan Wang, and Xinchao Wang. Mm-vet: Evaluating large multimodal models for integrated capabilities. arXiv preprint arXiv:2308.02490, 2023.
- [47] Xiang Yue, Yuansheng Ni, Kai Zhang, Tianyu Zheng, Ruoqi Liu, Ge Zhang, Samuel Stevens, Dongfu Jiang, Weiming Ren, Yuxuan Sun, Cong Wei, Botao Yu, Ruibin Yuan, Renliang Sun, Ming Yin, Boyuan Zheng, Zhenzhu Yang, Yibo Liu, Wenhao Huang, Huan Sun, Yu Su, and Wenhui Chen. Mmmu: A massive multi-discipline multimodal understanding and reasoning benchmark for expert agi. <https://arxiv.org/abs/2311.16502>, 2023. Accessed: 2025-05-14.
- [48] Rowan Zellers, Yonatan Bisk, Ali Farhadi, and Yejin Choi. From recognition to cognition: Visual commonsense reasoning. In *Proceedings of the IEEE/CVF Conference on Computer Vision and Pattern Recognition (CVPR)*, pages 6720–6730, 2019.

A Basic Settings

Figure 6 provides a comprehensive summary of the **MMLU-Reason** benchmark, including task type distributions, instance counts, and sub-category breakdowns. The benchmark consists of 1,083 multi-modal reasoning tasks spanning six high-level domains: Logic, Math, Space-Time, Code, Map, and Science. Each domain contains diverse subtypes (e.g., deductive logic, algebraic manipulation, spatial tracking, etc.), designed to probe distinct reasoning faculties. The chart further reports the proportion of each task type, ensuring balanced but realistic coverage aligned with real-world reasoning demands.

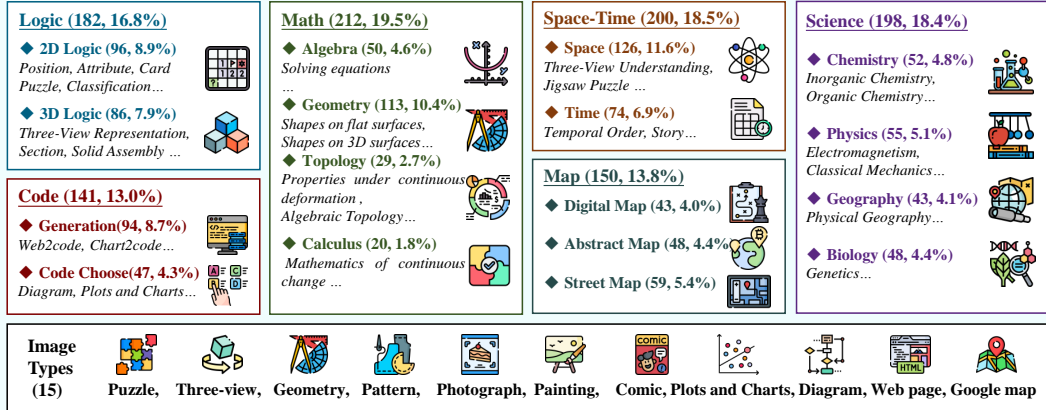


Figure 6: Task-type distribution and sub-category breakdown across the **MMLU-Reason** benchmark.

Expert Baselines. To contextualize the capabilities of MLLMs and MLLMs-T, we introduce two upper-bound baselines referred to as *Experts*, representing different degrees of human involvement:

- **Expert (Human only):** This setting represents pure human reasoning without any model assistance. We selected three co-authors of this paper, each with graduate-level expertise in AI, cognitive science, or related fields, to independently solve the benchmark tasks. Participants were provided with full task descriptions and multi-modal inputs (text and images), but were not exposed to model outputs or allowed external tools. To ensure reliability, each sample was independently answered by at least two annotators; disagreements were resolved via majority voting. The inter-annotator agreement, measured by Krippendorff's alpha, reached 0.84, indicating high consistency and shared task understanding.
- **Expert (Human + GPT-4o):** This hybrid configuration simulates a human-in-the-loop decision-support paradigm, where the same human experts were allowed to optionally consult GPT-4o during task resolution. Annotators first formed an independent judgment, then optionally queried GPT-4o for additional insights or solutions. Final responses reflected either acceptance or revision of GPT-4o's suggestions, along with justifications. This setting measures the upper bound of human-AI collaboration in structured reasoning tasks.

These expert configurations serve as practical performance ceilings: the human-only setting captures unaided expert cognition, while the hybrid setting reflects augmented performance with access to state-of-the-art MLLM support. Together, they frame the evaluation of MLLMs within a broader continuum of human-machine reasoning capabilities.

B Prompt Design

B.1 Base

Prompt Example. Base's prompt example is as follows:

Base's prompt example

Zero-shot Prompt:

- {question}
- {choice}

Please provide the final answer and store it in **\boxed{answer}**.

Critique Prompt: Review your previous answer and find problems with your answer.

Improve Prompt: Based on the problems you found, improve your answer. Please reiterate your answer, with your final answer a single numerical number, In the form **\boxed{answer}**.

B.2 Thinking Prompt

Prompt Example. The Thinking prompt is as follows:

Thinking Prompt Example

- {question}
- {choice}

Please think deeply before your response.

Please provide the final answer and store it in **\boxed{answer}**.

B.3 Image-text to Text Prompt

Prompt Example. The Image-text to text prompt is as follows:

Image-text to Text Prompt Example

- Based on the question and the image, please summary it in pure text. Just summary the question and image as detailed as possible, no need to give the answer.

B.4 Random Choice Baseline

Implementation Logic. The logic for the Random Choice baseline is as follows:

Random Choice Baseline Logic

```
def random_choice_baseline(questions, output_file):  
    with open(output_file, 'w', encoding='utf-8') as f_out:  
        for q in questions:  
            n = len(q["choices"])  
            labels = [chr(ord('A') + i) for i in range(n)]  
            prediction = random.choice(labels)  
            correct = normalize_answer(q["correct"])  
  
            result = {  
                "question": q.get("question", ""),  
                "prediction": prediction,  
                "correct": correct  
            }  
            f_out.write(json.dumps(result, ensure_ascii=False))
```

B.5 Frequent Choice Baseline

Implementation Logic. The logic for the Frequent Choice baseline is as follows:

Frequent Choice Baseline Logic

```
def frequent_choice_baseline(questions, output_file):
    counter = Counter()
    for q in questions:
        correct = normalize_answer(q["correct"])
        if correct:
            counter[correct] += 1

    if not counter:
        print("No valid answers found for frequent choice baseline. Skip.")
        return

    most_common_choice, _ = counter.most_common(1)[0]

    with open(output_file, 'w', encoding='utf-8') as f_out:
        for q in questions:
            correct = normalize_answer(q["correct"])
            result = {
                "question": q.get("question", ""),
                "prediction": most_common_choice,
                "correct": correct
            }
            f_out.write(json.dumps(result, ensure_ascii=False))
```

C Case Study

1. Logic: Thinking Case	18
2D Logic: Non-Thinking Case	19
3D Logic: Non-Thinking Case	20
2. Code: Thinking Case	21
Generation: Non-Thinking Case	22
Code Choose: Non-Thinking Case	23
3. Math: Thinking Case	24
Algebra: Non-Thinking Case	25
Geometry: Non-Thinking Case	26
Topology: Non-Thinking Case	27
Calculus: Non-Thinking Case	28
4. Space-Time: Thinking Case	29
Space Reasoning: Non-Thinking Case	30
Time: Non-Thinking Case	31
5. Map: Thinking Case	32
Route Plan: Non-Thinking Case	33
Street Map: Non-Thinking Case	34
6. Science: Thinking Case	35
Chemistry: Non-Thinking Case	36
Physics: Non-Thinking Case	37
Geography: Non-Thinking Case	38
Biology: Non-Thinking Case	39

Logical-Reasoning: 2D Logic

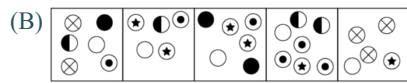
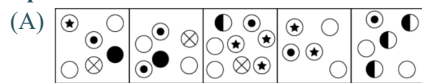
Question: Which set does the Figure belong to? Select from A, B, and C.

Image: <image 1>

<image 1>



Options:



(C) Neither set A nor set B

Thinking (From Claude-3.7):

I. Interpreting the Visual Problem

This is a pattern classification task with:

Set A (top row): 5 boxes. Set B (middle row): 5 boxes. Figure (bottom): 1 box to classify as Set A, Set B, or neither.

II. Extracting Symbolic Features

Set A Characteristics:

Symbols include: stars (★), filled circles (●), empty circles (○), half-filled circles (◐), and X marks (☒). Notable variation exists in both symbol count and distribution.

Set B Characteristics:

Same symbol set appears. Need to identify what differentiates Set B from Set A.

Bottom Figure Composition:

2 stars (★) 2 empty circles (○) 1 half-filled circle (◐) 0 filled circles (●) 0 X symbols (☒)

III. Comparative Symbol Analysis

Counted symbol distributions per box:

Set A:

	Set B:
A1: ★×1, ●×2, ○×3, ◐×0, ☒×2	B1: ★×0, ●×1, ○×1, ◐×1, ☒×3
A2: ★×0, ●×2, ○×3, ◐×0, ☒×1	B2: ★×2, ●×0, ○×2, ◐×1, ☒×0
A3: ★×3, ●×1, ○×2, ◐×1, ☒×1	B3: ★×2, ●×2, ○×1, ◐×0, ☒×0
A4: ★×2, ●×2, ○×2, ◐×0, ☒×0	B4: ★×1, ●×3, ○×1, ◐×2, ☒×0
A5: ★×0, ●×1, ○×3, ◐×2, ☒×0	B5: ★×1, ●×0, ○×1, ◐×0, ☒×3

The Figure:

★×2, ●×0, ○×2, ◐×1, ☒×0

Observation: The Figure's symbol composition exactly matches Set B box 2.

IV. Symbol Count Comparison

Set A: 6–8 symbols Set B: 5–7 symbols Figure: 5 symbols → fits Set B

V. Conclusion

The Figure's total symbol count and exact match with Set B box 2 confirm its classification.

Correct Answer: A

Response: Looking at this problem, the goal is to determine which set the bottom figure belongs to—Set A, Set B, or neither.

The figure contains: 2 stars (★), 2 empty circles (○), 1 half-filled circle (◐), No filled circles (●) or X symbols (☒)

Set B, box 2, has an identical symbol composition, and its total symbol count (5) also matches that of the figure. Set A boxes typically contain more symbols and different combinations.

Given the perfect match in both symbol type and count, the figure clearly **belongs to Set B.**

Figure 7: Logic: Thinking Case

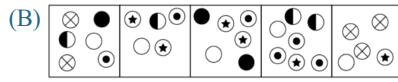
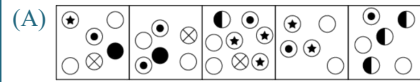
Logical-Reasoning: 2D Logic

Question: Which set does the Figure belong to? Select from A, B, and C.
Image: <image 1>



<image 1>

Options:



(C) Neither set A nor set B

Correct Answer: A

Response: Looking at this problem, the goal is to determine which set the bottom figure belongs to—Set A, Set B, or neither.

The figure contains: 2 stars (★), 2 empty circles (○), 1 half-filled circle (◐), No filled circles (●) or X symbols (✗)

Set B, box 2, has an identical symbol composition, and its total symbol count (5) also matches that of the figure. In contrast, Set A boxes typically contain more symbols and different combinations.

Given the perfect match in both symbol type and count, the figure clearly **belongs to Set B.**



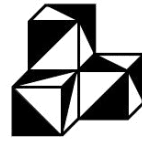
Figure 8: 2D Logic: Non-Thinking Case

Logical Reasoning: 3D Logic

Question: For the following three-dimensional figures, which of the four options cannot be its view (front view, top view, side view)?

Image: <image 1>

Options:



<image 1>

Correct Answer: D

Response: I'll analyze this problem step by step to determine which of the four options cannot be a valid view of the three-dimensional figure shown at the top.

Let me examine the 3D figure at the top of the image. It appears to be composed of cubic blocks arranged in a specific configuration with black and white triangular patterns on each visible face. To solve this problem, I need to mentally visualize what this 3D object would look like from different viewing angles (front, top, and side views) and compare these with the four options labeled A, B, C, and D.

When I examine a 3D cube-based object from orthogonal directions:

- Each face should show a distinct 2D projection.
- The patterns on visible faces should match the black and white triangular patterns shown in the original figure.
- The overall shape should be consistent with the 3D arrangement of blocks.

Looking carefully at each option:

Option A: This shows an L-shaped arrangement with specific black/white triangular patterns that could represent a valid view of the 3D figure.

Option B: This shows a rectangular arrangement with triangular patterns that could represent a valid view from certain angles.

Option C: This shows a T-shaped arrangement with triangular patterns.

Option D: This shows a zigzag arrangement with triangular patterns.

When I visualize the 3D structure from various angles, I notice that option D shows a pattern that cannot be derived from the given 3D figure. The specific arrangement of blocks and triangular patterns in option D is inconsistent with any possible orthographic projection (front, top, or side) of the 3D structure shown.

Therefore, **option D cannot be a valid view of the three-dimensional figure.**



Figure 9: 3D Logic: Non-Thinking Case

Code: Code Generation

Question: This is a matrix traversal problem where we need to: - Start from the top-right corner of a given matrix- Follow a specific spiral pattern in counter-clockwise direction. - Collect all elements in the order of traversal- The traversal pattern should work for matrices of different sizes (M x N). # Visual Facts: Four example matrices are shown with different dimensions:

- 4x1 (top-right)
- 4x2 (top-left)
- 4x3 (bottom-left)
- 4x4 (bottom-right).

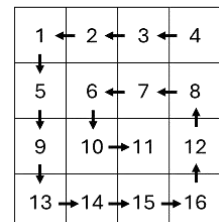
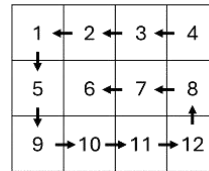
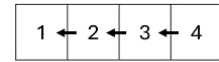
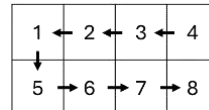
.....

Visual Patterns:

1. Movement Direction Pattern:.....
2. Traversal Rules:.....

Please provide the final answer and store it in `\boxed{answer}`.

Image: <Image 1>



<Image 1>

Correct Answer: *****

Response:

Matrix Spiral Traversal Algorithm:

Based on the problem description and visual examples, I need to create an algorithm that traverses a matrix in a counter-clockwise spiral starting from the top-right corner.

Solution:

The key is to follow the directional pattern (Left \u2192 Down \u2192 Right \u2192 Up) and change direction whenever we hit a boundary or previously visited cell.

'''python

def spiral_traverse(matrix):

.....

Example:

For a 3x3 matrix:'''
1 2 3
4 5 6
7 8 9'''



Figure 10: Code: Thinking Case

Code: Code Generation

Question: This is a matrix traversal problem where we need to: - Start from the top-right corner of a given matrix- Follow a specific spiral pattern in counter-clockwise direction. - Collect all elements in the order of traversal- The traversal pattern should work for matrices of different sizes (M x N). # Visual Facts: Four example matrices are shown with different dimensions:

- 4x1 (top-right)
- 4x2 (top-left)
- 4x3 (bottom-left)
- 4x4 (bottom-right)

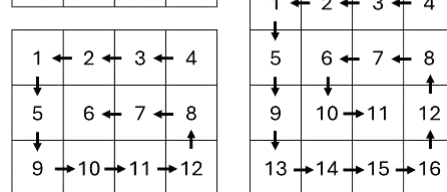
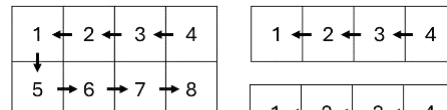
.....

Visual Patterns:

1. Movement Direction Pattern:.....
2. Traversal Rules:.....

Please provide the final answer and store it in `\boxed{answer}`.

Image: <Image 1>



<Image 1>

Thinking (From Claude-3.7):

This problem is asking me to write code for a spiral matrix traversal, starting from the top-right corner and moving in a counter-clockwise direction. From the visual examples and description, I can see that:

1. We start at the top-right corner (0, N-1)
2. Initial direction is leftward
3. When we reach a boundary or a cell, we change direction in a counter-clockwise manner
4. The direction sequence is: Left \u2192 Down \u2192 Right \u2192 Up \u2192 Left \u2192 ...
5. We need to collect all elements in the order of traversal
6. The algorithm should work for any MxN matrix

Let me design an algorithm for this:.....

Here's a pseudo-code representation:.....



Correct Answer: *****

Response:

Matrix Spiral Traversal Algorithm:

Based on the problem description and visual examples, I need to create an algorithm that traverses a matrix in a counter-clockwise spiral starting from the top-right corner.

Solution:

The key is to follow the directional pattern (Left \u2192 Down \u2192 Right \u2192 Up) and change direction whenever we hit a boundary or previously visited cell.

```python

```
def spiral_traverse(matrix):
```

.....

### Example:

For a 3x3 matrix:```1 2 3\n4 5 6\n7 8 9```



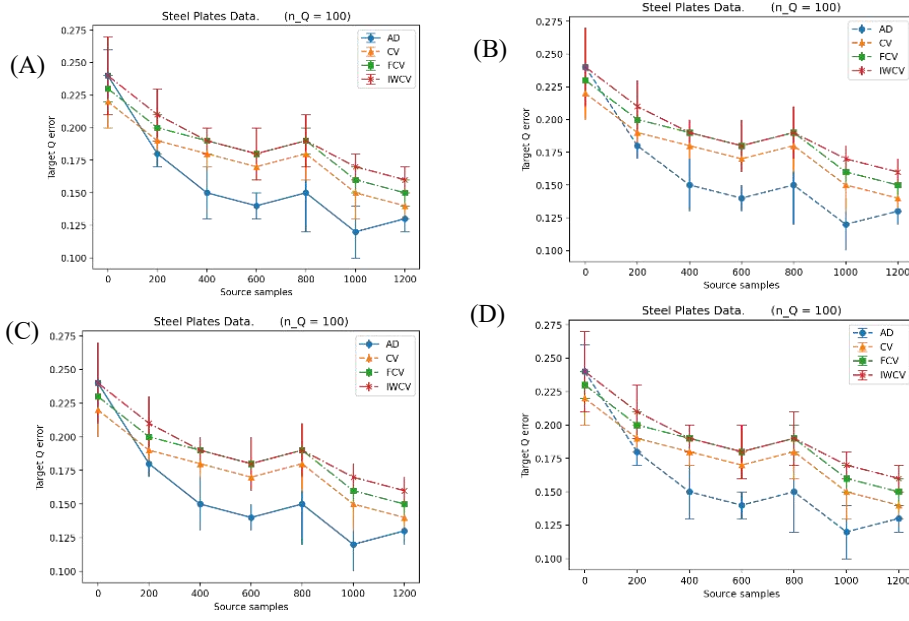
Figure 11: Generation: Non-Thinking Case

## Code: Code Choose

**Question:** Which visualization can this code possibly generate? We are using Python version 3.11.0, matplotlib version 3.6.3, and seaborn version 0.12.2 (if applicable).

```
import matplotlib.pyplot as plt.....
provide the final answer and store it in \boxed{answer}.
```

**Options:**



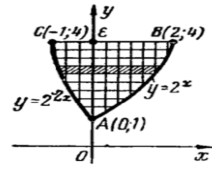
**Correct Answer: D**

**Response:** Visualization Analysis: Looking at the Python code and comparing it with the provided images, I can determine which visualization this code would generate. The code creates an error bar plot. Among the provided images, the **first image** most closely matches what this code would generate. It accurately shows:- The correct line styles (dashed for AD and CV, dash-dot for FCV and IWCV)- The proper markers (circles, triangles, squares, and x marks)- Error bars with the specified cap size- The exact title, axis labels, and legend positioning. The other images have either slight differences in line styling, marker appearance, or rendering issues (like the last image which has text corruption at the bottom).



Figure 12: Code Choose: Non-Thinking Case

**Question:** <image 1> Find the surface area bounded by the curves  $y=2x$ ,  $y=2^{-2x}$  and  $y=4$ .  
**image:** <image 1>



<image 1>

**Thinking (From Claude-3.7):**

I. **Identify Intersection Points**

The intersections are found to be A(0,1) from  $y=2^x$  and  $y=2^{-2x}$ ; B(2,4) from  $y=2^x$  and  $y=4$ ; and C(-1,4) from  $y=2^{-2x}$  and  $y=4$ .

II. **Define the Integration Strategy and Set Up Integrals**

The lower boundary is  $y=2^{-2x}$  for  $-1 \leq x \leq 0$  and  $y=2^x$  for  $0 \leq x \leq 2$ , leading to:  $\text{Area} = \int_0^{-1} 4 - 2^{-2x} dx + \int_0^2 4 - 2^x dx$ .

III. **Evaluate the Integrals**

The first integral solved by u-substituting  $2^{-2x}$  term, resulting  $4 - 3/(2\ln(2))$   
 The second integral is computed with result of  $8 - 3/\ln(2)$

IV. **Finalize the Answer**

Summing up the two integrals gives the total area as  $12 - 9/(2\ln(2))$



**Correct Answer:  $24 - 9/(2\ln(2))$**

**Response:** To find the area bounded by the curves  $y=2^x$ ,  $y=2^{-2x}$ , and  $y=4$ , the first step was to identify their intersection points, which were determined to be A(0,1), B(2,4), and C(-1,4). These points define the vertices of the region. The area calculation was then set up by dividing the region at  $x=0$ , recognizing that  $y=4$  is the upper boundary, while the lower boundary changes from  $y=2^{-2x}$  (for  $x$  between -1 and 0) to  $y=2^x$  (for  $x$  between 0 and 2). This led to expressing the total area as the sum of two definite integrals:  $\int_0^{-1} 4 - 2^{-2x} dx + \int_0^2 4 - 2^x dx$ . The first integral, corresponding to the left portion, was evaluated to  $4 - 3/(2\ln(2))$ , involving a u-substitution for the exponential term. The second integral, for the right portion, was evaluated to  $8 - 3/(2\ln(2))$ . Finally, summing these two results yielded the total enclosed area as  $12 - 9/(2\ln(2))$ .

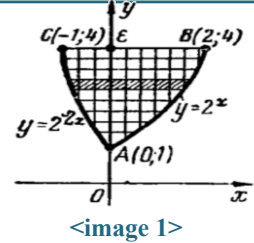


Figure 13: Math: Thinking Case

## Math: Calculus

**Question:** <image 1> Find the surface area bounded by the curves  $y=2^x$ ,  $y=2^{-x}$  and  $y=4$ .

**Image:** <image 1>



<image 1>

**Correct Answer:**  $24 - 9/(2\ln(2))$

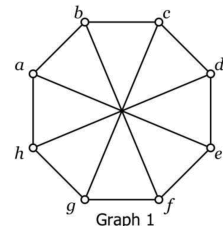
**Response:** To find the area bounded by the curves  $y=2^x$ ,  $y=2^{-x}$ , and  $y=4$ , the first step was to identify their intersection points, which were determined to be  $A(0,1)$ ,  $B(2,4)$ , and  $C(-1,4)$ . These points define the vertices of the region. The area calculation was then set up by dividing the region at  $x=0$ , recognizing that  $y=4$  is the upper boundary, while the lower boundary changes from  $y=2^{-x}$  (for  $x$  between -1 and 0) to  $y=2^x$  (for  $x$  between 0 and 2). This led to expressing the total area as the sum of two definite integrals:  $\int_0^{-1} 4 - 2^{-x} dx + \int_0^2 4 - 2^x dx$ . The first integral, corresponding to the left portion, was evaluated to  $4 - 3/(2\ln(2))$ , involving a u-substitution for the exponential term. The second integral, for the right portion, was evaluated to  $8 - 3/(2\ln(2))$ . Finally, summing these two results yielded the total enclosed area as  $12 - 9/(2\ln(2))$ .



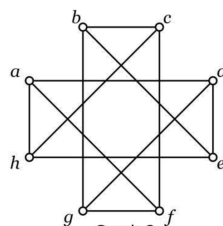
Figure 14: Algebra: Non-Thinking Case

**Question:** Which of the following graphs are not isomorphic?

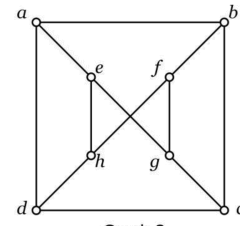
**Options:**



(A)



(B)



(C)

**Correct Answer: A**

**Response: A, B, C**

Isomorphism requires a one-to-one mapping between vertices that preserves adjacency.

Graph 1 is described as a wheel graph with a central hub, where each of the 8 vertices has a degree of 3, making it a regular graph.

Graph 2 has a more rectangular structure with diagonals. Its vertices have degrees of either 3 or 4, resulting in a degree sequence of  $\{3, 4, 3, 4, 4, 3, 4, 3\}$ . This differing degree sequence immediately indicates that Graph 2 is not isomorphic to Graph 1 or Graph 3.

Graph 3 forms a square with internal vertices. All 8 of its vertices have a degree of 3, resulting in a regular graph with a degree sequence of  $\{3, 3, 3, 3, 3, 3, 3, 3\}$ .

Further comparison between Graph 1 and Graph 3 reveals structural differences. Graph 1's wheel-like structure with a central hub maintains connectivity upon removal of any single vertex. In contrast, removing specific vertices in Graph 3's square-based structure would disconnect the graph. This difference in connectivity properties confirms that Graph 1 and Graph 3 are not isomorphic.

Therefore, based on their degree sequences and structural properties, none of the three graphs are isomorphic to each other.

**Final Answer: A, B, C**



Figure 15: Geometry: Non-Thinking Case

## Math: Geometry

**Question:** A  $4 \times 4 \times h$  rectangular box contains a sphere of radius  $2$  and eight smaller spheres of radius  $1$ . The smaller spheres are each tangent to three sides of the box, and the larger sphere is tangent to each of the smaller.

**Image:** <image 1>

**Options:**

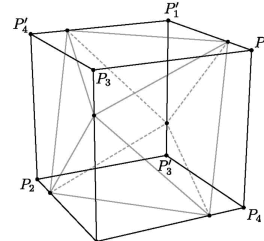
(A):  $\frac{3\sqrt{2}}{4}$

(B):  $\frac{7\sqrt{6}}{16}$

(C):  $\frac{\sqrt{5}}{2}$

(D):  $\frac{2\sqrt{3}}{3}$

(E)  $\frac{\sqrt{6}}{2}$



<image 1>

**Correct Answer: A**

**Response:**  $\sqrt{2}$

Consider a unit cube. We aim to find the side length of a regular octahedron with vertices on the cube's edges:  $P_1, P_2, P_3, P_4, P_1', P_2', P_3',$  and  $P_4'$ . By symmetry, the octahedron's vertices can be at  $(t,0,0), (0,t,0), (0,0,t), (1-t,1,1), (1,1-t,1),$  and  $(1,1,1-t)$ . For a regular octahedron, all edges are equal. The distance between adjacent vertices, e.g.,  $(t,0,0)$  and  $(0,t,0)$ , is  $t\sqrt{2}$ . The distance between opposite vertices, e.g.,  $(t,0,0)$  and  $(1-t,1,1)$ , is  $\sqrt{(2t-1)^2 + 2}$ . Equating adjacent edge lengths,  $t\sqrt{2} = t\sqrt{4t^2 - 4t + 3}$ , leads to a quadratic with no real solutions for  $t$ . However, considering the geometry, a regular octahedron inscribed with vertices at the midpoints of the edges of a cube with side length  $s$  has a side length of  $\frac{s}{\sqrt{2}} * \sqrt{2} = s$ . For our unit cube  $s=1$ , this is not the case here as vertices are on the edges, not necessarily midpoints. Through geometric reasoning and the symmetry of the problem, the regular octahedron formed by these conditions has a side length where the distance between adjacent vertices is  $\sqrt{(t-0)^2 + (0-t)^2 + (0-0)^2} = t\sqrt{2}$ . By symmetry and the properties of a regular octahedron inscribed in this manner, the side length is determined to be  $\sqrt{2}$ .

**Final Answer: The side length is  $\sqrt{2}$ .**



Figure 16: TopoLogic: Non-Thinking Case

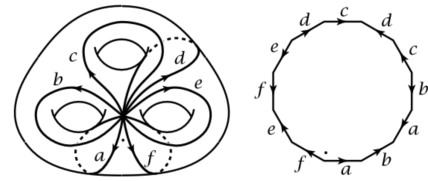
## Math: Topology

**Question:** Considering the provided diagram depicting a surface and its associated fundamental group, which of the following group presentations accurately represents the fundamental group of the surface shown in the left part of the diagram?

**Image:** <image 1>

**Options:**

- (A)  $\langle a, b, c, d, e, f \mid aba^{-1}b^{-1}cdc^{-1}d^{-1}efe^{-1}f^{-1} = 1 \rangle$
- (B)  $\langle a, b, c, d, e, f \mid abcd = ef, a = b^{-1}, c = d^{-1}, e = f^{-1} \rangle$
- (C)  $\langle a, b, c, d, e, f \mid abcdef = 1 \rangle$
- (D)  $\langle a, b, c, d, e, f \mid ab^{-1}cd^{-1}ef^{-1} = 1 \rangle$



<image 1>

**Correct Answer: B**

**Response: C**

The left figure shows a surface with a specific topological structure, and the right figure appears to be the boundary of this surface or a representation of loops that define the fundamental group.

When working with fundamental groups of surfaces using presentations, we need to identify how the boundary components are glued together. The standard approach is to understand how the edges are identified in pairs.

From the diagram, I can see that we have loops labeled a through f. The arrows indicate direction, and the identifications form the surface boundary.

In the canonical presentation of the fundamental group of a surface, the product of all commutators (for orientable surfaces) or all squares (for non-orientable surfaces) equals the identity. Alternatively, if we're looking at a surface with boundary, we'd have a relation that the product of all boundary elements equals the identity. Looking at the right diagram, it appears to show a polygon with edges labeled a through f, which when glued according to the labels and orientations, forms the surface on the left. The boundary word reading clockwise is  $abcdef$ . For a surface with a single boundary component, as this appears to be, the fundamental group would have the relation that the product of all boundary edges (read in order) equals the identity. Therefore, the presentation that correctly represents this surface is:  $\langle a, b, c, d, e, f \mid abcdef = 1 \rangle$ .

This corresponds to option (C).

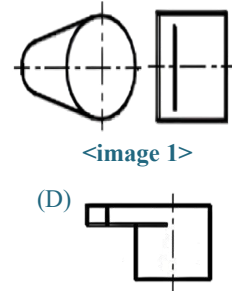


Figure 17: Calculus: Non-Thinking Case

## Space-Time: Space

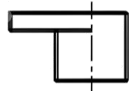
**Question:** Given the front view and left view of a solid, please choose the correct top view from options A, B, C, and D.

**Image:** <image 1>



**Options:**

(A)



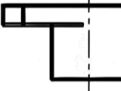
(B)



(C)



(D)



### Thinking (From Claude-3.7):

#### I. Interpreting Provided Views

Front View (left): \*\*\*. Left View (right): \*\*\*.

#### II. Extracting Critical Features

Front View Observations: \*\*\*. Left View Observations: \*\*\*.

#### III. Reconstructing the 3D Object

Mapping Curvature from Front View: \*\*\*. Validating Depth from Left View: \*\*\*.

#### IV. Evaluating Top View Candidates

- ❑ Option A features a uniform L-shape but fails to account for the width gradation observed in the oval profile of the front view. → **eliminate**;
- ❑ Option B adopts a horizontally expanded L-configuration, reflecting the oval's maximum width at its horizontal centerline as depicted in the front view. → **keep**;
- ❑ Option C incorporates a stepped horizontal edge, introducing geometric complexity not supported by the original front or left views. → **eliminate**;
- ❑ Option D proposes a narrowed horizontal base, which directly conflicts with the oval's widening trend visible in the front view. → **eliminate**.

#### V. Concluding the Analysis

**The answer is B.**



### Correct Answer: B

**Response:** For the correct top view, it must be consistent with both the front and left views; The vertical centerline should align with the same features in all views; The shape must account for the oval profile seen in the front view.

The oval in the front view indicates that when viewed from the top, we should see a part with varying width. Option B matches this expectation because: 1) Its wider horizontal section corresponds to the wider part of the oval in the front view. 2) The straight vertical line on the left matches the flat profile seen in the left view. 3) The overall L-shape explains how the object can appear oval from the front while rectangular from the left. **Therefore, the correct top view is B.**



Figure 18: Space-Time: Thinking Case

## Space-Time: Space

**Question:** <image 1> Select the correct arrangement from the options below to reconstruct the original image. Each option defines the subfigure positions as [top-left, top-right, bottom-left, bottom-right].

**Image:** <image 1>

**Options:**

- A. [4, 2, 1, 3], B. [2, 3, 1, 4],
- C. [1, 3, 4, 2], D. [4, 1, 3, 2].



<image 1>

### Correct Answer: D

**Response:** To determine the correct arrangement of the subfigures, we need to analyze the content and logical placement of each subfigure in the context of a typical auditorium layout.

Subfigure 1: This image shows a close-up view of the seating area with steps leading up to the seats. It appears to be a detailed view of the lower section of the auditorium.

Subfigure 2: This image shows an elevated view of the auditorium, capturing both the seating area and the ceiling structure. It seems to be taken from a higher vantage point, possibly from the balcony.

Subfigure 3: This image focuses on the ceiling and upper part of the auditorium, showing the lighting and architectural details of the ceiling.

Subfigure 4: This image provides a broader view of the seating area, similar to Subfigure 1 but from a slightly different angle and with more of the floor visible.

Given these observations, we can deduce the following:

Top-left (position 1): This should be a view that provides a good overview but is not the most detailed or highest vantage point. Subfigure 4 seems suitable here as it gives a broad view of the seating area.

Top-right (position 2): This should be a higher vantage point view, which is best represented by Subfigure 2.

Bottom-left (position 3): This should be a detailed view of a specific part, such as the ceiling or a section of the seats. Subfigure 3, which shows the ceiling details, fits well here.

Bottom-right (position 4): This should be a detailed view of the seating area, which is best represented by Subfigure 1.

Thus, the correct arrangement is [4, 2, 3, 1].

However, the options provided are: A. [4, 2, 1, 3] B. [2, 3, 1, 4] C. [1, 3, 4, 2] D. [4, 1, 3, 2]

Comparing our deduced arrangement [4, 2, 3, 1] with the given options, the closest match is Option A: [4, 2, 1, 3].

**Therefore, the final answer is A.**



Figure 19: Space Reasoning: Non-Thinking Case

## Space-Time: Time

**Question:** Which frame appears first on the match timeline?

**Options:**

(A)



(B)



**Correct Answer: B**

**Response:** To determine which frame appears first on the match timeline, we need to analyze the sequence of events in both images.

Image A:

The ball is in the air, approaching the goal. The goalkeeper is preparing to make a save. Players are positioned around the goal area, with some running towards the ball.

Image B:

The ball is on the ground, closer to the goalkeeper. The goalkeeper appears to be in the process of making a save or has just made contact with the ball. Players are still around the goal area, but their positions suggest a slightly earlier moment in the action compared to Image A.

In Image B, the ball is on the ground and closer to the goalkeeper, indicating an earlier moment in the sequence. In Image A, the ball is in the air, suggesting it has already been kicked and is approaching the goal, which occurs after the scenario in Image B.

**Therefore, Image B appears first on the match timeline.**

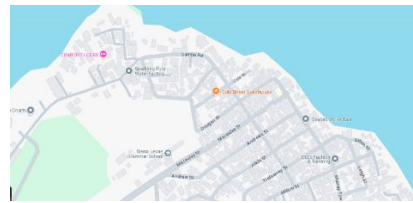


Figure 20: Time: Non-Thinking Case

## Map: Route Plan

**Question:** How to get to Sierra Leone Grammer School from Seabird Water Taxi after having lunch at Cole Street Guesthouse? Please provide the final answer and store it in \boxed{answer}.

**Image:** <image 1>



<image 1>

**Options:**

- A. Seabird Water Taxi. Head northwest on High Broad St toward Andrews ....
- B. Seabird ...St.Turn left onto Andrews St Continue onto Andrew St.Turn right onto Macaulay St.Sierra Leone Grammar School
- C. ...Leone Grammar School. Head northeast on Macaulay St. Turn left at the 1st cross street toward Cole St. Turn left at the 2nd cross street onto Cole St .Cole Street Guesthouse
- D. ...Cole St toward Damba Rd. Turn right at the 1st cross street toward Macaulay St. Sierra Leone Grammar School

**Thinking(From Claude-3.7):**

Let me analyze each option to see which describes this specific journey:

**Option 1** includes:- Directions from Seabird Water ...

**Option 2** only includes:- Directions from Seabird ....

**Option 3** includes:- Directions from Seabird ....

**Option 4** includes:- Directions from Seabird Water Taxi to Cole Street Guesthouse- Followed by directions from Cole Street Guesthouse to Sierra Leone Grammar School.

**This is the route we need!** The second part describes how to get from Cole Street Guesthouse to Sierra Leone Grammar School.



**Correct Answer: D**

**Response:**

# Directions from Cole Street Guesthouse to Sierra Leone Grammar School. Looking at the map and analyzing the provided options, I need to determine the correct route from Cole Street Guesthouse to Sierra Leone Grammar School (after having lunch at Cole Street Guesthouse). Based on the map, ...These directions provide the most efficient route from Cole Street Guesthouse to Sierra Leone Grammar School according to the map layout.



Figure 21: Map: Thinking Case

## Map: Route Plan

**Question:** How to get to Sierra Leone Grammer School from Seabird Water Taxi after having lunch at Cole Street Guesthouse? Please provide the final answer and store it in \boxed{answer}.

**Image:** [Image 1](#)



**<image 1>**

**Options:**

- A. Seabird Water Taxi. Head northwest on High Broad St toward Andrews St. Turn left onto Andrews St. Continue onto Andrew St. Turn right onto Macaulay St. Sierra Leone Grammar School. Head northeast on Macaulay St. Turn left at the 1st cross street toward Cole St. Turn left at the 2nd cross street onto Cole St. Cole Street Guesthouse.
- B. Seabird Water Taxi. Head northwest on High Broad St toward Andrews St. Turn left onto Andrews St  
Continue onto Andrew St. Turn right onto Macaulay St. Sierra Leone Grammar School
- C. Seabird Water Taxi. Head northwest on High Broad St toward Andrews St. Turn left onto Macaulay St. Sierra Leone Grammar School. Head northeast on Macaulay St. Turn left at the 1st cross street toward Cole St. Turn left at the 2nd cross street onto Cole St. Cole Street Guesthouse
- D. Seabird Water Taxi. Head northwest on High Broad St toward Andrews St. Turn right toward Cole St. Turn left at the 1st cross street onto Cole St. Cole Street Guesthouse. Head northeast on Cole St toward Damba Rd. Turn right at the 1st cross street toward Macaulay St. Turn right at the 2nd cross street onto Macaulay St. Sierra Leone Grammar School

### **Correct Answer: D**

#### **Response:**

Directions from Cole Street Guesthouse to Sierra Leone Grammar School. Looking at the map and analyzing the provided options, I need to determine the correct route from Cole Street Guesthouse to Sierra Leone Grammar School (after having lunch at Cole Street Guesthouse). Based on the map, I can see that Cole Street Guesthouse is located on Cole Street in the northeastern area, while Sierra Leone Grammar School is situated near Macaulay Street in the southwestern portion of the map. After examining all the options, the correct directions would be: \boxed{Head northeast on Cole St toward Damba Rd. Turn right at the 1st cross street toward Macaulay St. Turn right at the 2nd cross street onto Macaulay St. Sierra Leone Grammar School}. These directions provide the most efficient route from Cole Street Guesthouse to Sierra Leone Grammar School according to the map layout.



Figure 22: Route Plan: Non-Thinking Case

## Map: Street Map

**Question:** The autonomous vehicle is currently in the center lane of a six-lane divided urban road, as verified from the forward and top-down views. The visible arrow markings indicate that this lane supports only forward motion, while the adjacent right lane supports both straight and right-turn maneuvers. The vehicle is approaching a signal-controlled intersection approximately 80 meters ahead, where a right turn is required for route compliance. However, the right lane currently has a motorcycle and another vehicle positioned closely, potentially creating a dynamic obstacle during the lane-change maneuver. The surrounding environment features consistently spaced trees and streetlights, confirming lane widths of approximately 3.5 meters and indicating symmetrical roadside geometry, as seen in the left-back and right-back views. The autonomous system must decide whether to immediately initiate a right lane change or maintain position temporarily. Given that lane changes require a minimum gap of 20 meters in the target lane and take 4 seconds to complete safely at 36 km/h, which of the following is the most contextually appropriate \*\*decision-making strategy\*\* for this scenario? Please provide the final answer and store it in `\boxed{answer}`.

**Image:** [Image 1](#)

[Image 1](#)



### Options:

- A. Initiate lane change immediately to secure position before potential blockage
- B. Wait until within 30 meters of the intersection, then merge quickly
- C. Slow down to create a gap and merge once rear vehicle clears
- D. Proceed forward and reroute at the next available legal right turn

### Correct Answer: C

#### Response:

According to the scenario:

- The vehicle needs to make a right turn at the upcoming intersection.
- The intersection is approximately 80 meters ahead.
- Lane changes require a minimum 20-meter gap.
- Lane changes take 4 seconds to complete at 36 km/h.
- There are vehicles in the right lane that may create obstacles.

Evaluating the options:

- Option A (immediate lane change) would be risky with vehicles currently in the right lane.
- Option B (waiting until 30 meters before intersection) leaves minimal room for error.
- Option C (slowing down to create a gap) is safest and most pragmatic.
- Option D (proceeding and rerouting) is unnecessary given other viable options.

The most appropriate strategy would be to slow down slightly, allowing the vehicles in the right lane to proceed, then safely merge once there's sufficient space, which aligns with option C.



Figure 23: Street Map: Non-Thinking Case

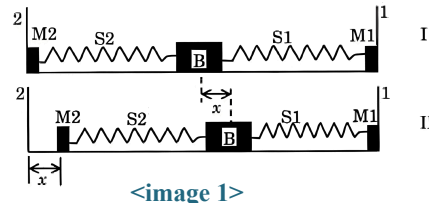
## Science: Physics

**Question:** A block  $B$  is connected to two unstretched springs with spring constants  $k$  and  $4k$ . The block is displaced a distance  $x$  to the left from equilibrium and released. It then moves a maximum distance  $y$  to the right. Find the ratio  $y/x$ .

**Image:** <image 1>

**Options:**

(A) 4    (B) 2    (C) 1/2    (D) 1/4



<image 1>

### Thinking (From Claude-3.7):

#### I. Interpreting Provided Views

Figure I shows the system at equilibrium with both springs unstretched. Figure II shows block B displaced a distance  $x$  toward wall 1.

#### II. Extracting Critical Features

Supports M1 and M2 are massless and free to move, so they adjust to keep the net force on them zero. The energy is entirely stored in the springs when the block is displaced.

#### III. Reconstructing the System Dynamics

At displacement  $x$ :

$$E_{\text{initial}} = (1/2) * k * x^2 + (1/2) * (4k) * x^2 = (5/2) * k * x^2$$

At maximum displacement  $y$  on the other side:

$$E_{\text{final}} = (5/2) * k * y^2$$

Conservation of energy gives:

$$(5/2) * k * x^2 = (5/2) * k * y^2 \rightarrow y = x$$

#### IV. Evaluating Physical Consistency

The system is isolated with no external forces; the center of mass remains stationary. Since the supports are massless, their movement does not contribute to the system's inertia or momentum. Thus, the motion is symmetric, and the block oscillates equally about the equilibrium point.

#### V. Concluding the Analysis

The answer is:  $y/x = 1$ .



### Correct Answer: 1/2

**Response:** The system consists of a block connected to two springs: one with spring constant  $k$  and the other with  $4k$ . The supports can move freely, and the system is frictionless. When the block is displaced by a distance  $x$  toward wall 1 and released, the total potential energy stored in both springs is:  $E_{\text{initial}} = (1/2) \cdot k \cdot x^2 + (1/2) \cdot 4k \cdot x^2 = (5/2) \cdot k \cdot x^2$ .

At the maximum displacement  $y$  on the opposite side, both springs are again stretched (or compressed), and the total energy is:  $E_{\text{final}} = (1/2) \cdot k \cdot y^2 + (1/2) \cdot 4k \cdot y^2 = (5/2) \cdot k \cdot y^2$ . By conservation of mechanical energy (since there is no friction),  $(5/2) \cdot k \cdot x^2 = (5/2) \cdot k \cdot y^2 \rightarrow x^2 = y^2 \rightarrow y = x$ . **Thus, the ratio  $y/x = 1$ .**

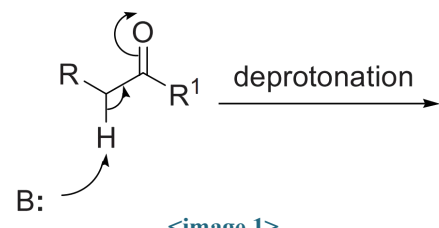


Figure 24: Science: Thinking Case

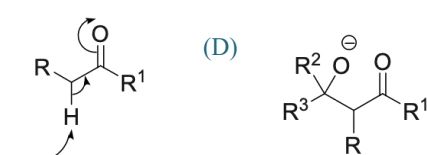
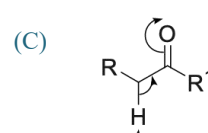
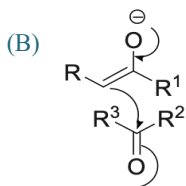
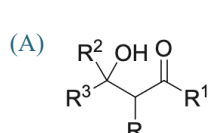
## Science: Chemistry

**Question:** The transition-state structure changes after electron relocation or reaction. Which of the following options shows the structure after the change?

**Image:** <image\_1>



**Options:**



**Correct Answer: D**

**Response:** For the correct product after the deprotonation step in Image 1, we must identify the immediate consequence of removing the alpha hydrogen from a carbonyl compound. The carbonyl (C=O) group adjacent to an alpha hydrogen undergoes deprotonation by a base, forming an enolate ion. This ion has a delocalized negative charge between the oxygen of the carbonyl and the alpha carbon. Image 5 correctly represents this enolate structure: 1) The negative charge is shown on the oxygen, consistent with resonance stabilization. 2) The carbon-carbon double bond has shifted accordingly to reflect enolate formation. 3) Other options either show further reaction products (Image 2 and Image 3) or the unchanged starting material (Image 4).

Therefore, the correct immediate product after deprotonation is shown in D.

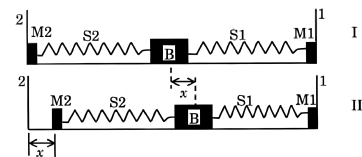


Figure 25: Chemistry: Non-Thinking Case

## Science: Physics

**Question:** A block  $B$  is connected to two unstretched springs with spring constants  $k$  and  $4k$ . The block is displaced a distance  $x$  to the left from equilibrium and released. It then moves a maximum distance  $y$  to the right. Find the ratio  $y/x$ .

**Image:** [image 1](#)



[image 1](#)

**Options:** (A) 4 (B) 2 (C) 1/2 (D) 1/4

**Correct Answer: 1/2**

**Response:** The system consists of a block connected to two springs: one with spring constant  $k$  and the other with  $4k$ . The supports can move freely, and the system is frictionless. When the block is displaced by a distance  $x$  toward wall 1 and released, the total potential energy stored in both springs is:  $E_{\text{initial}} = (1/2) \cdot k \cdot x^2 + (1/2) \cdot 4k \cdot x^2 = (5/2) \cdot k \cdot x^2$ . At the maximum displacement  $y$  on the opposite side, both springs are again stretched (or compressed), and the total energy is:  $E_{\text{final}} = (1/2) \cdot k \cdot y^2 + (1/2) \cdot 4k \cdot y^2 = (5/2) \cdot k \cdot y^2$ . By conservation of mechanical energy (since there is no friction),  $(5/2) \cdot k \cdot x^2 = (5/2) \cdot k \cdot y^2 \rightarrow x^2 = y^2 \rightarrow y = x$ .

**Thus, the ratio  $y/x = 1$ .**



Figure 26: Physics: Non-Thinking Case

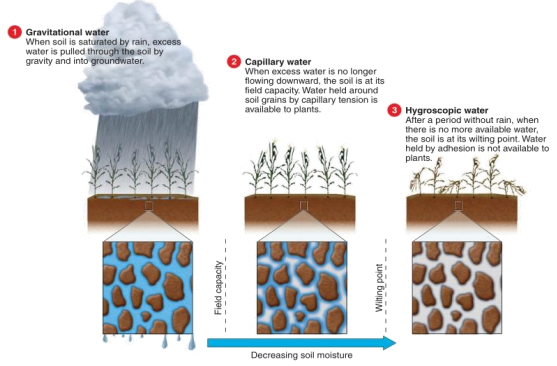
## Science: Geography

**Question:** Which water in <image 1> coats soil particles? It's largely unavailable to plants, held tightly by strong molecular forces.

**Image:** <image 1>

**Options:**

- (A) Gravitational water
- (B) Capillary water
- (C) Hygroscopic water



<image 1>

**Correct Answer: (C)**

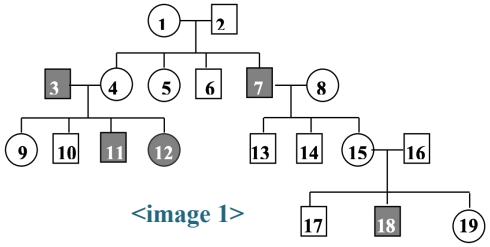
**Response:** To identify the type of water that is tightly bound to soil particles and unavailable to plants, we examine how soil water is categorized. Water in soil exists in three main forms: gravitational, capillary, and hygroscopic. Hygroscopic water forms a very thin layer around soil particles and is held by strong adhesive forces. These forces are so intense that plants cannot extract this water, and it does not evaporate under normal conditions. In contrast, gravitational water drains quickly, and capillary water is available to plants.

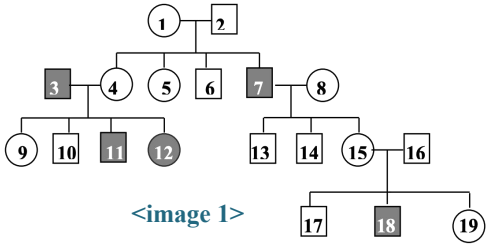
**Therefore, the water that is firmly attached to soil particles and unavailable to plants is hygroscopic water.**



Figure 27: Geography: Non-Thinking Case

## Science: Biology

**Question:** In pedigree  of a Gene A - related disease (non - shaded in - married individuals are non - carriers, complete penetrance), what is Individual 9's genotype?

**Image:** 

**Options:**

(A) AA      (B) Aa      (C) Aa or AA      (D)  $X^AX^A$   
 (E)  $X^AX^a$       (F)  $X^AX^A$       or      (G)  $X^aX^a$

**Correct Answer: E**

**Response:** To determine the genotype of Individual 9, we analyze the pedigree and identify the mode of inheritance. The disease appears in every generation and affects both males and females, indicating an autosomal dominant pattern. In this pattern, affected individuals must carry at least one dominant disease allele (A), while unaffected individuals are homozygous recessive (aa). Individual 9 is not shaded, meaning they do not express the disease phenotype. This implies they do not carry the dominant allele and must have the genotype aa.

**Therefore, the correct genotype of Individual 9 is aa.**



Figure 28: Biology: Non-Thinking Case